nature plants

ARTICLES

PUBLISHED: 5 OCTOBER 2015 | ARTICLE NUMBER: 15140 | DOI: 10.1038/NPLANTS.2015.140

An RLP23–SOBIR1–BAK1 complex mediates NLP-triggered immunity

Isabell Albert[1‡], Hannah Böhm[1‡], Markus Albert[1], Christina E. Feiler[1], Julia Imkampe[1], Niklas Wallmeroth[1], Caterina Brancato[1], Tom M. Raaymakers[2], Stan Oome[2,3†], Heqiao Zhang[4], Elzbieta Krol[5], Christopher Grefen[1], Andrea A. Gust[1], Jijie Chai[4], Rainer Hedrich[5], Guido Van den Ackerveken[2,3] and Thorsten Nürnberger[1*]

Plants and animals employ innate immune systems to cope with microbial infection. Pattern-triggered immunity relies on the recognition of microbe-derived patterns by pattern recognition receptors (PRRs). Necrosis and ethylene-inducing peptide 1-like proteins (NLPs) constitute plant immunogenic patterns that are unique, as these proteins are produced by multiple prokaryotic (bacterial) and eukaryotic (fungal, oomycete) species. Here we show that the leucine-rich repeat receptor protein (LRR-RP) RLP23 binds *in vivo* to a conserved 20-amino-acid fragment found in most NLPs (nlp20), thereby mediating immune activation in *Arabidopsis thaliana*. RLP23 forms a constitutive, ligand-independent complex with the LRR receptor kinase (LRR-RK) SOBIR1 (Suppressor of Brassinosteroid insensitive 1 (BRI1)-associated kinase (BAK1)-interacting receptor kinase 1), and recruits a second LRR-RK, BAK1, into a tripartite complex upon ligand binding. Stable, ectopic expression of RLP23 in potato (*Solanum tuberosum*) confers nlp20 pattern recognition and enhanced immunity to destructive oomycete and fungal plant pathogens, such as *Phytophthora infestans* and *Sclerotinia sclerotiorum*. PRRs that recognize widespread microbial patterns might be particularly suited for engineering immunity in crop plants.

Higher eukaryotes employ germline-encoded PRRs to recognize microbial patterns and to activate antimicrobial defences[1,2]. Microbe-derived triggers of host immunity are collectively termed pathogen-associated molecular patterns (PAMPs)[3,4]. Plants utilize large sets of PRRs for microbial pattern sensing and activation of PAMP-triggered immunity (PTI)[1,2,5]. Host-adapted microbes have evolved effectors to suppress PTI[6]. Co-evolution of host plants and pathogens has shaped effector-triggered immunity (ETI), which is initiated mainly by cytoplasmic immune receptors that recognize either effector structures or effector-mediated manipulations of host targets[7]. Immune receptors implicated in both, ETI and PTI, mediate microbial pattern recognition and plant immune activation[8].

Plant PRRs are plasma membrane proteins, many of which carry LRR ectodomains[1]. LRR PRRs predominantly mediate recognition of proteinaceous microbial patterns. LRR domains are either linked via transmembrane domains to cytoplasmic receptor kinase domains (LRR-receptor kinase PRRs, LRR-RKs) or to short cytoplasmic tails lacking apparent signalling domains (LRR-receptor protein PRRs, LRR-RPs)[2,5]. *Arabidopsis* FLS2 and EFR are LRR-RKs that recognize bacterial flagellin (flg22) or elongation factor Tu (elf18), respectively[9,10]. LRR-RPs comprise fungal pattern sensors Cf-4 (refs. 11,12), Eix2 (ref. 13), Ve1 (ref. 14) (from tomato), RLP30 (ref. 15), RLP42 (ref. 16) (from *Arabidopsis*), the bacterial pattern sensor RLP1 (ref. 17) (from *Arabidopsis*) and the oomycete elicitin sensor ELR from potato[18].

PRRs mediate pattern binding and initiation of intracellular signal transduction[1,2,5]. As LRR-RPs lack cytoplasmic domains, receptor/co-receptor complex formation is instrumental for LRR-RP-mediated signal transmission[5]. *Arabidopsis* and tomato LRR-RPs interact in a constitutive, ligand-independent fashion with the LRR-RK SOBIR1[5,15,16,19]. LRR-RP SOBIR1 heteromeric complexes have been proposed to be functionally equivalent to genuine LRR-RKs[5]. Although compelling, this proposition yet awaits experimental confirmation.

LRR-RKs interact in a ligand-dependent manner with members of the SERK (SOMATIC EMBRYOGENESIS RECEPTOR KINASE) protein family, including SERK3/BAK1 and SERK4/BKK1 (ref. 20). Genetic evidence supports negative and positive regulatory roles of BAK1 in LRR-RP-mediated immunity. BAK1 attenuates fungal xylanase-induced immune activation through tomato Eix2 (ref. 21), while *Arabidopsis* RLP30 (ref. 15) and tomato Cf-4-mediated immune activation[22] was impaired in *bak1* mutants. Ligand-induced biochemical complex formation of LRR-RP SOBIR1 complexes with BAK1 has, however, not been demonstrated.

NLPs form a superfamily of microbial proteins produced by bacterial, fungal and oomycete species[23,24]. NLPs have been discovered as cytotoxic proteins triggering leaf necrosis and plant immunity-associated defences in dicotyledonous plants[23,25]. Recently, non-cytotoxic NLPs were found in oomycete and fungal species, suggesting functional diversification within eukaryotic species producing NLPs[26–28]. A conserved 20-mer fragment (nlp20) is sufficient for immune activation by cytotoxic and non-cytotoxic NLPs in various *Brassicaceae* species including *Arabidopsis*[29,30]. Many of the 1,100 NLP-encoding sequences deposited in databases harbour this motif and are likely active triggers of plant defences[29]. Prokaryotic and eukaryotic species from three microbial lineages produce nlp20-containing NLPs. This uniquely broad taxonomic

[1]Center of Plant Molecular Biology (ZMBP), University of Tübingen, Auf der Morgenstelle 32, Tübingen D-72076, Germany. [2]Plant-Microbe Interactions, Department of Biology, Utrecht University, Padualaan 8, Utrecht 3584 CH, The Netherlands. [3]Centre for BioSystems Genomics (CBSG), Wageningen, The Netherlands. [4]Tsinghua-Peking Center for Life Sciences, School of Life Sciences, Tsinghua University, Beijing 100084, China. [5]Department of Plant Physiology and Biophysics, University of Würzburg, Julius-von-Sachs-Platz 2, Würzburg D-97082, Germany. †Present address: Averis Seeds BV, Valthermond, The Netherlands. ‡These authors contributed equally to this work. *e-mail: nuernberger@uni-tuebingen.de

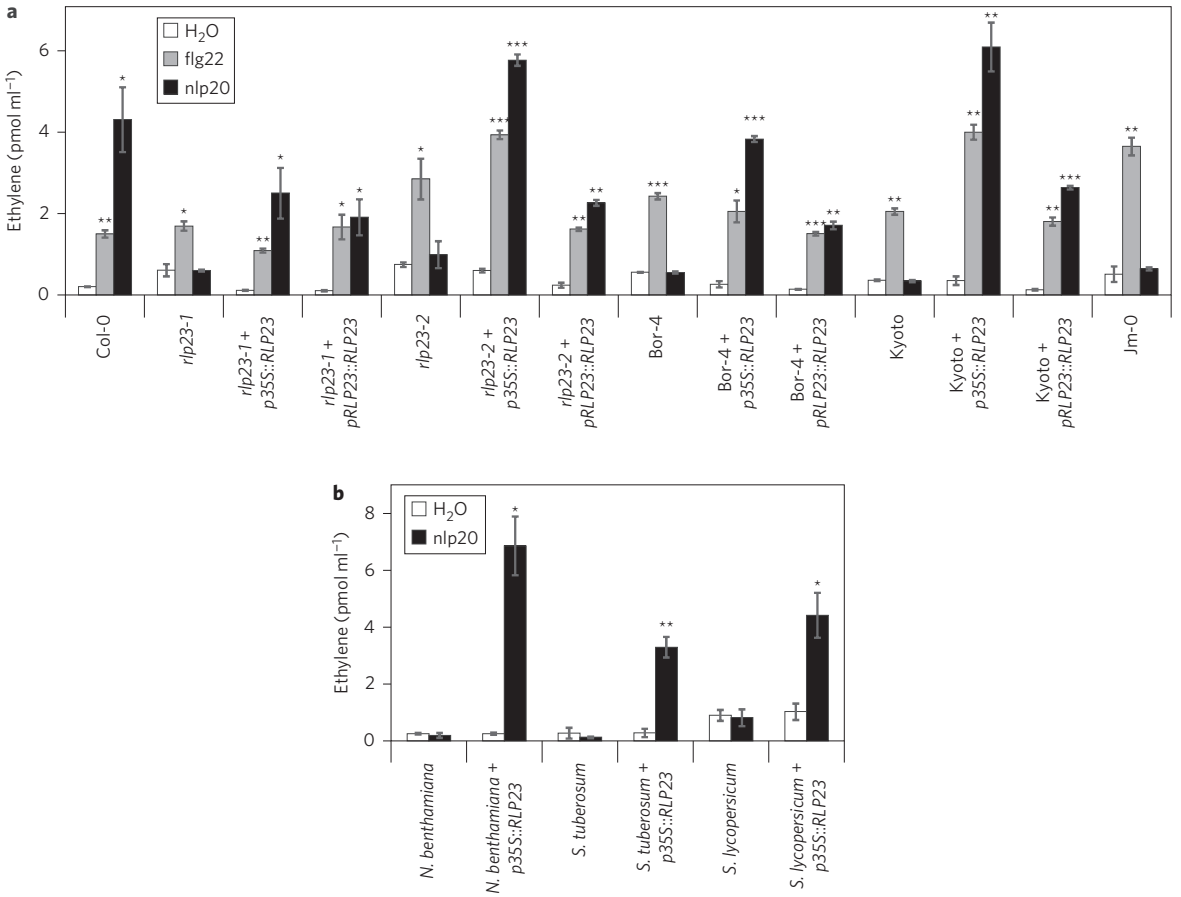

Figure 1 | RLP23 confers sensitivity to nlp20. a,**b**, Ethylene accumulation after treatment with 1 μM nlp20, flg22 or water as control in *A. thaliana* mutants, nlp20-insensitive accessions and in stably transformed *Arabidopsis p35S::RLP23–GFP* transgenic plants (**a**), and in stably transformed *p35S::RLP23–GFP* transgenic *N. benthamiana*, *S. tuberosum* and *S. lycopersicum* plants (**b**). Bars represent means ± s.d. of three replicates. Asterisks indicate significant differences to water control treatments (*$P < 0.05$, **$P < 0.01$, ***$P < 0.001$, Student's *t*-test). Experiments were performed three times with similar results.

distribution is unmatched by any known trigger of metazoan or plant immunity[29,30].

We report on an RLP23–SOBIR1–BAK1 complex that mediates nlp20 sensing and immune activation in *Arabidopsis*. We show that interfamily transfer of RLP23 confers nlp20 sensitivity to solanaceous plants and that ectopic expression in potato enhances immunity to devastating phytopathogens, such as *Phytophthora infestans* and *Sclerotinia sclerotiorum*.

Results

RLP23 mediates nlp20 recognition. Plant LRR-type PRRs predominantly mediate recognition of proteinaceous ligands[2]. To identify the *Arabidopsis* nlp20 receptor, LRR-RK and LRR-RP transfer DNA (t-DNA) insertion mutant collections (Col-0)[31,32] were tested for nlp20-inducible ethylene production (Supplementary Fig. 1). Whereas 38 mutant genotypes representing 29 different LRR-RKs proved sensitive to nlp20 treatment, *rlp23–1* and *rlp23-2* alleles lacking expression of the gene encoding RLP23 (At2g32680; ref. 32) lacked nlp20-sensitivity (Fig. 1a and Supplementary Fig. 1). Sensitivity to flg22 was unaltered in *rlp23* mutants, suggesting that these plants are specifically impaired in nlp20-mediated immunity (Fig. 1a). In parallel, 135 *Arabidopsis* accessions were screened for nlp20 responsiveness (Supplementary Fig. 2). Three accessions (Bor-4, Jm-0, Kyoto) proved insensitive to nlp20, but not to flg22, again suggesting signal-specific impairment of nlp20 recognition (Fig. 1a). nlp20 sensitivities varied quantitatively among the accessions tested. Whether this is due to polymorphisms in *RLP23* alleles remains to be shown.

RLP23 comprises an ectodomain of 27 LRR units interspersed by an island domain separating LRRs 22/23, juxtamembrane and transmembrane domains and a cytosolic 17-amino-acid tail (Supplementary Fig. 3a). Inspection of genomic *RLP23* sequences in nlp20-insensitive *Arabidopsis* accessions revealed the same frame-shift mutation within LRR13 resulting in premature TAG stop codons (Supplementary Fig. 3a) and lack of nlp20 sensitivity (Fig. 1a). Loss of nlp20 pattern recognition occurs rather rarely as only three of 135 accessions tested were found to be nlp20-insensitive.

A causal link between the presence of RLP23 and nlp20 sensitivity was established when a *p35S::RLP23–GFP* (green fluorescent protein) construct was expressed in *Nicotiana benthamiana* plants (Supplementary Fig. 3c). Non-transformed plants were insensitive to nlp20 (Fig. 1b)[29]. In contrast, *RLP23–GFP*-expressing plants recognized nlp20 in a dose-dependent manner and at concentrations as low as 10 nM (Supplementary Fig. 3c). Expression of the frame-shift *rlp23 (Bor-4)* allele fused to GFP neither conferred nlp20 sensitivity nor resulted in RLP23–GFP protein accumulation (Supplementary Fig. 3d,e). Stable expression of *p35S::RLP23–GFP* in *Arabidopsis rlp23-1* or *rlp23-2* mutants restored nlp20 sensitivity (Fig. 1a). Likewise, stable expression of *pRLP23::RLP23–GFP* also conferred nlp20-inducible ethylene production to *rlp23-1* and *rlp23-2* genotypes as well as to nlp20-insensitive accessions Bor-4 and Kyoto (Fig. 1a). Further, stable expression of *p35S::RLP23–GFP* in *N. benthamiana*, potato (*Solanum tuberosum*) or tomato (*Solanum lycopersicum*) resulted in RLP23 production (Supplementary Fig. 4) and nlp20 sensitivity (Fig. 1b). Altogether,

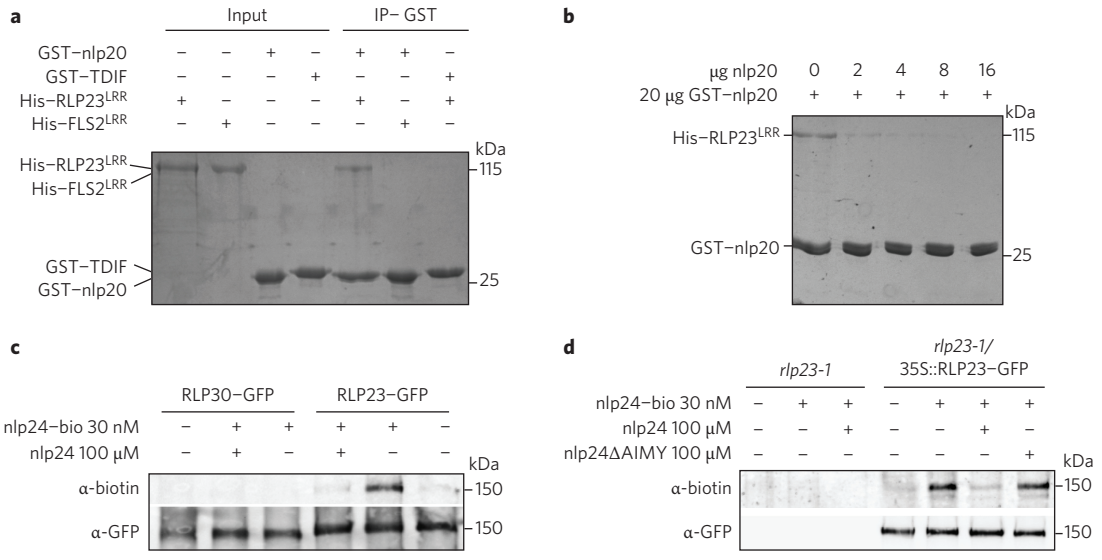

Figure 2 | nlp20 interacts specifically with RLP23 *in vitro* a,b and *in planta* c,d. a,**b**, SDS–PAGE/Coomassie analysis of the interaction of recombinant GST–nlp20 and recombinant His-tagged RLP23^{LRR} and FLS2^{LRR} domains (**a**), and competition of GST–nlp20 binding by increasing amounts of untagged nlp20 (**b**). GS4B resin-bound GST-tagged fusion proteins were used to precipitate recombinant LRR protein. **c**,**d**, Protein blot analysis of proteins obtained by cross-linking assays using RLP23–GFP as receptor, biotinylated nlp24 (nlp24-bio) as ligand and non-biotinylated nlp24 as competitor of ligand binding in *N. benthamiana* plants transiently expressing RLP23–GFP (**c**) and in stably transformed 35S::RLP23–GFP *A. thaliana* plants (**d**). Excess of an inactive nlp20 variant (nlp24ΔAIMY)[29] was used as a negative control (**d**). *N. benthamiana* plants transiently expressing RLP30–GFP[15] (**c**) and *rlp23-1 A. thaliana* mutants (**d**) served as negative controls. GFP-trap beads were used for co-immunoprecipitation and protein blots were probed with anti-biotin antisera, stripped and re-probed with GFP-antisera. Representative examples selected from three independent repetitions are shown.

these findings demonstrate that RLP23 is required for nlp20 pattern recognition, and that RLP23 confers pattern-specific immune activation to insensitive *Arabidopsis* accessions and to various solanaceous species.

Rapid plasma membrane depolarization is one of the fastest responses in *Arabidopsis* cells when treated with LRR-RK PRR ligands, such as flg22 (refs 33,34). Substantial alterations in the membrane potential were observed also within 2 min of addition of nlp20 that were not detectable when either an elicitor-inactive nlp20 derivative (nlp20_W6A; ref. 29) or when cells from *rlp23-1* mutants were tested (Supplementary Fig. 5a,b). nlp20 concentrations required to evoke half-maximum membrane depolarization (ΔV_{max} = 126.5 ± 7.4 mV) were 2.77 ± 0.74 nM and thus similar to half-maximum effective concentration (EC_{50}) values determined for ethylene production (Supplementary Fig. 5c)[29,30]. This is the first report on pattern-triggered membrane depolarization mediated by an LRR-RP PRR.

nlp20-inducible reactive oxygen species (ROS) accumulation, callose apposition and MAPK activation detected in Col-0 plants were abolished in *rlp23-1* and *rlp23-2* genotypes (Supplementary Fig. 6a–c). Likewise, nlp20-related peptides from oomycete (*Hyaloperonospora arabidopsidis*, *Ha*NLP3), fungal (*Botrytis cinerea*, *Bc*NEP2) or bacterial NLPs (*Bacillus subtilis*, *Bs*NPP1)[29,30] triggered ethylene production in Col-0 plants, but not in *rlp23*-1 mutants (Supplementary Fig. 6d).

The RLP23 LRR domain interacts physically with nlp20. LRR domains of plant PRRs interact physically with their cognate peptide patterns[2]. Recombinant RLP23 LRR ectodomains (RLP23^{LRR}) and glutathione *S*-transferase (GST)-tagged nlp20 were used to analyse binding *in vitro*. GST–nlp20 fusion protein precipitated recombinant RLP23^{LRR}, but not a recombinant FLS2 LRR ectodomain (Fig. 2a). GST fused with a peptide structurally unrelated to nlp20 (GST–tracheary element differenciation inhibitory factor (TDIF)) failed to precipitate the RLP23 ectodomain. Likewise, addition of increasing concentrations of soluble nlp20 together with GST–nlp20 competitively reduced amounts of precipitated RLP23^{LRR} (Fig. 2b), suggesting that RLP23 and nlp20 interact specifically and directly. To analyse ligand–receptor binding *in planta*, nlp24-bio (Supplementary Fig. S7)[29] was used as a ligand. nlp24 is biologically as active as nlp20 (ref. 29) and comprises the nlp20 sequence and four additional C-terminal amino acid residues of *Pp*NLP in front of the biotin tag. This larger ligand was chosen to rule out potentially negative effects of the tag on the biological activity of the nlp20 peptide. Leaves of *p35S::RLP23–GFP*-expressing *N. benthamiana* (Fig. 2c) or of *Arabidopsis* plants (Fig. 2d) were treated with nlp24-bio before treatment with a homo-bifunctional chemical cross-linker, EGS (ethylene glycol bis-succinimidyl succinate). Subsequently, RLP23–GFP protein was precipitated and analysed for ligand binding. Binding of nlp24-bio to RLP23–GFP was detected in both plant species. Ligand concentrations used were similar to those required for its biological activity (Supplementary Fig. 7)[29], suggesting physiological significance of binding. Large excess of free nlp24 competitively abolished binding of nlp24-bio, demonstrating ligand specificity (Fig. 2c,d). Use of a biologically inactive nlp24 derivative (nlp24ΔAIMY)[29] did not affect nlp24-bio binding to RLP23–GFP (Fig. 2d). Likewise, binding assays performed in *N. benthamiana* expressing a structurally related LRR-RP, RLP30 (ref. 15), or in the *Arabidopsis rlp23-1* mutant did not show binding, suggesting that RLP23 specifically binds nlp peptides.

RLP23 function requires LRR-RKs SOBIR1 and BAK1. As RLP23 lacks an apparent cytoplasmic signalling domain, RLP23-dependent immune activation likely requires a co-receptor for intracellular signalling. To identify RLP23-interacting proteins, *p35S::RLP23–GFP* was stably expressed in the *rlp23-1* genotype. Protein extracts prepared from mock-treated plants or from plants treated with nlp20 were subjected to co-precipitation assays using GFP-binding beads and subsequent MS/MS spectroscopy to identify RLP23–GFP interactors (Supplementary Fig. 8a). Among a total of 13 proteins found to interact with RLP23–GFP, only two

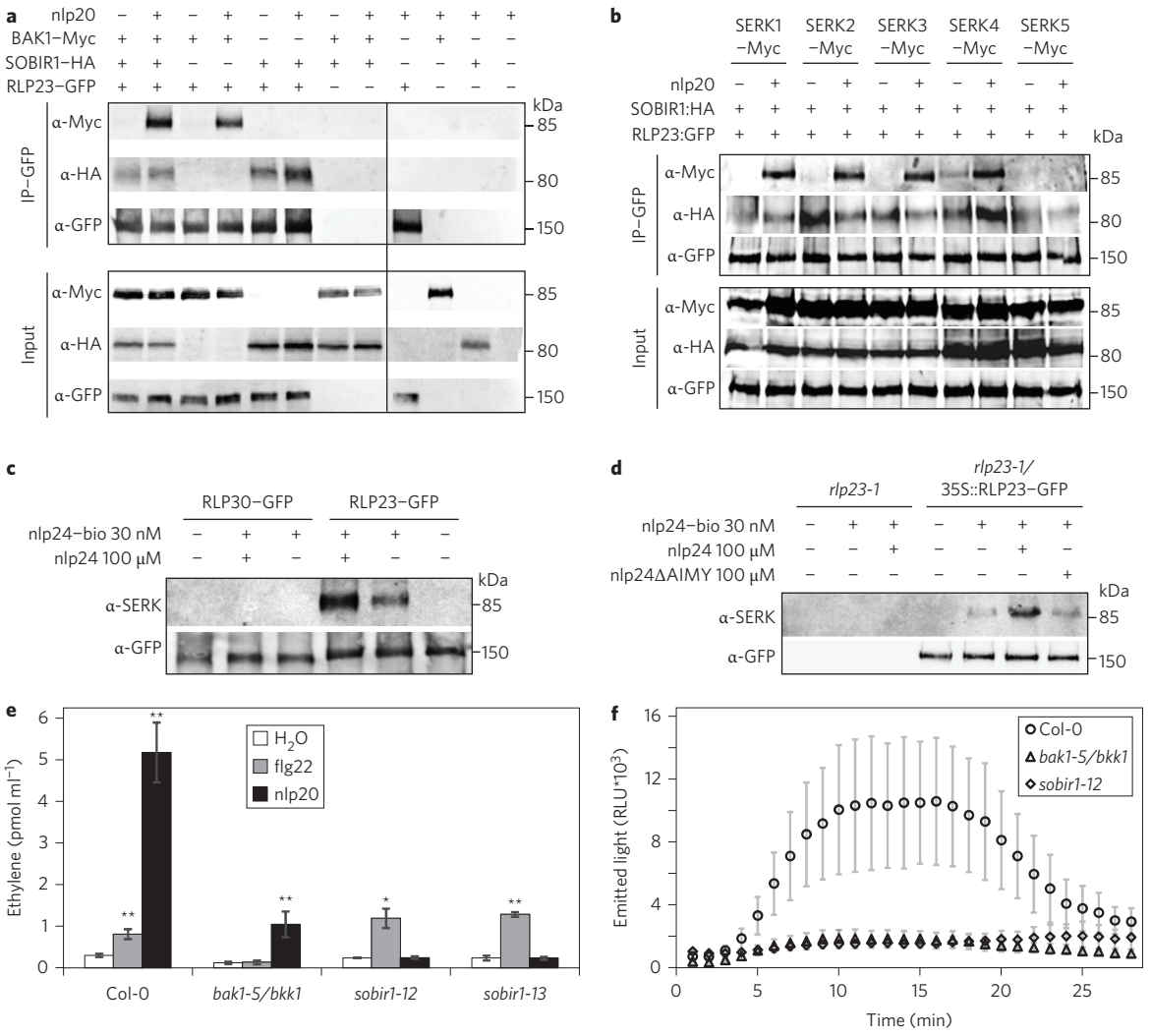

Figure 3 | RLP23 interacts with SOBIR1, BAK1 and other members of the SERK protein family, and these proteins are required for nlp20-mediated defence activation. a, RLP23–GFP, BAK1–Myc and SOBIR1–HA proteins were transiently expressed in *N. benthamiana*, protein extracts thereof subjected to co-immunoprecipitation using GFP-trap beads, and pelleted proteins were analysed by protein blotting using tag-specific antisera. **b**, Protein blot analysis of Myc-tagged SERK1, SERK2, SERK3/BAK1, SERK4/BKK1 and SERK5 proteins transiently co-expressed with SOBIR1–HA and RLP23–GFP in *N. benthamiana* and co-immunoprecipitated using GFP-trap beads. **c**,**d**, Protein blots from experiments shown in Fig. 2c,d were stripped and re-probed with anti-SERK-antiserum. **e**, Ethylene accumulation and **f**, oxidative burst measurements in *Arabidopsis sobir1* and *bak1-5/bkk1* mutants treated with nlp20 (1 µM), or water and flg22 (1 µM) as controls. Average values of three replicates ± s.d. are shown. Asterisks indicate significant differences to water control treatments (*$P < 0.05$, **$P < 0.01$, Student's *t*-test). Experiments were performed in triplicate with similar results.

potential co-receptors were detected. Fifteen peptides representing the LRR-RK SOBIR1 co-purified with RLP23 *in planta* independent of the presence of nlp20, confirming constitutive, ligand-independent interaction of RLP23 and SOBIR1 (ref. 35) (Supplementary Fig. 8b). In contrast, three peptides representing the LRR-RK, BAK1, were found only among proteins prepared from plants treated with nlp20 (Supplementary Fig. 8a,b). BAK1 is a co-receptor serving LRR-RKs (refs 2,20,36,37), but genetic evidence has recently implicated BAK1 also in LRR-RP function[14,15,21]. Co-immunoprecipitation experiments in *Arabidopsis rlp23-1/p35S::RLP23–GFP* transgenic plants confirmed nlp20-dependent interaction of RLP23 and BAK1 (Supplementary Fig. 8c). Likewise, similar assays conducted in *N. benthamiana* also showed ligand-independent interaction of RLP23 and SOBIR1 (Fig. 3a). Again, RLP23–BAK1 interaction was found solely in nlp20-elicited plants invariably of whether RLP23–GFP or SOBIR1–GFP fusion proteins were precipitated, thus confirming ligand-dependent complex formation (Fig. 3a and Supplementary Fig. 9a). Expression of a structurally related *Arabidopsis* LRR-RP, RLP30 (ref. 15), together with SOBIR1 and BAK1 resulted in RLP30–SOBIR1–BAK1 complex formation, again only when plants were treated with the RLP30 ligand, SCFE1 (ref. 15) (Supplementary Fig. 9b). Thus, ligand-dependent recruitment of BAK1 might be a common feature of LRR-RP-type PRRs.

Over-expression of four SERK protein family members (SERK1, SERK2, SERK3/BAK1, SERK4/BKK1) in *N. benthamiana* resulted in nlp20-induced RLP23–SERK complex formation (Fig. 3b), suggesting functional redundancy among SERK proteins. Protein blots obtained in Fig. 2c,d, were probed with anti-SERK antisera (Fig. 3c,d). Again, nlp20-dependent RLP23–SERK complexes were observed in *Arabidopsis* and *N. benthamiana*, suggesting that native SERK levels support ligand-dependent complex formation with LRR-RP-type PRRs.

To assess SOBIR1 and BAK1 functions in nlp20-induced immunity, *sobir1* and *bak1-5/bkk1* mutants were tested for nlp20-induced

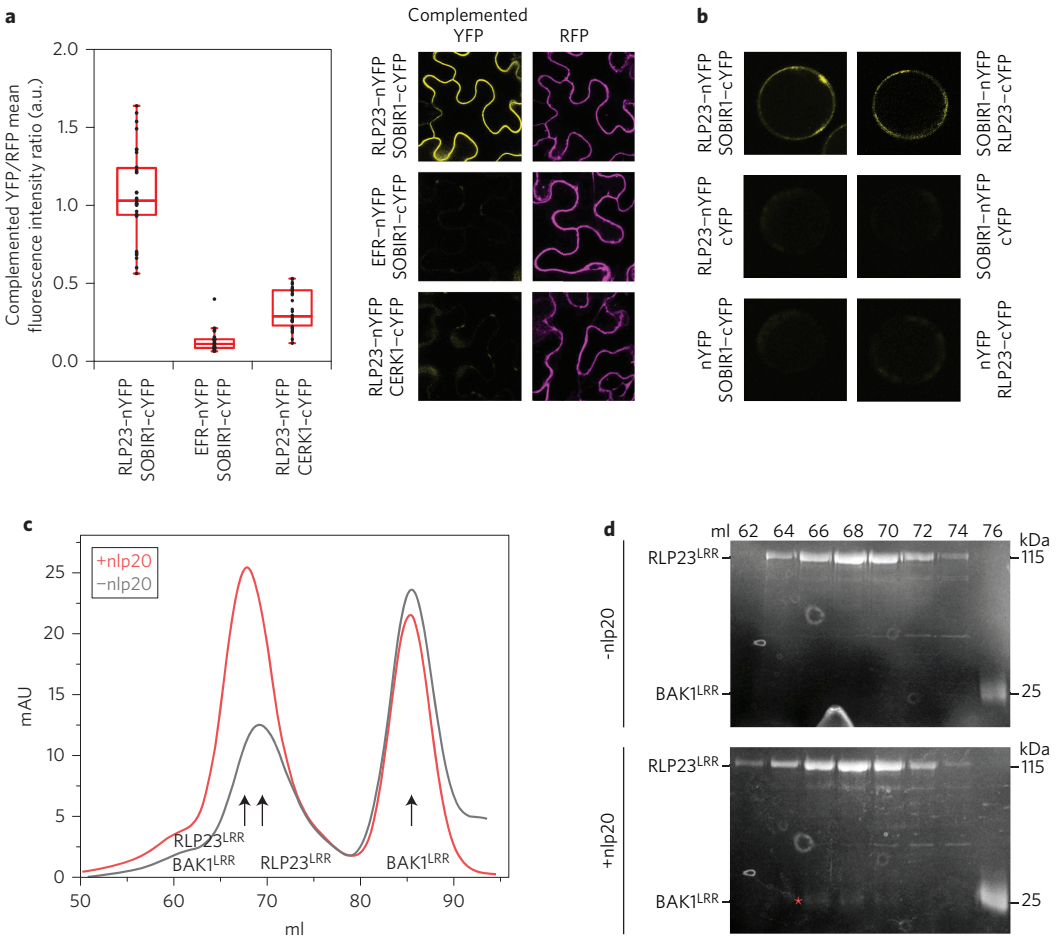

Figure 4 | RLP23 physically interacts with SOBIR1 and BAK1. a, RLP23 interacts with SOBIR1 in a ratiometric bimolecular fluorescence complementation analysis in transiently transformed *N. benthamiana* leaves. Mean fluorescence intensity of complemented YFP was ratioed against RFP signal in 30 randomly chosen square sections of approx. 9,500 μm², each. Box plot diagram depicting all individual values as black dots, 75th percentile as open square above and 25th percentile as open square below the red horizontal line which denotes the median value. Top and bottom whiskers comprise values within 1.5 times of the interquartile range (IQR). Exemplary confocal images of analysed samples; left, complemented YFP; right, cytosolic RFP fluorescence. **b**, Protoplasts of *A. thaliana* plants transiently expressing RLP23-nYFP and SOBIR1-cYFP or SOBIR1-nYFP and RLP23-cYFP show fluorescence of complemented YFP as observed by confocal laser scanning microscopy. As controls, nYFP and cYFP constructs only were used. **c**,**d**, Gel filtration experiment (Hiload 200, GE Healthcare) demonstrating ligand-induced complex formation of recombinant RLP23 and BAK1 ectodomains *in vitro* after pre-incubation of both receptor ectodomains with nlp20 for 20 min (**c**). Arrows indicate peak maximum positions of $BAK1^{LRR}$, $RLP23^{LRR}$ and $BAK1^{LRR}RLP23^{LRR}$ proteins. Fractions from (**c**) were subjected to SDS-PAGE/Coomassie blue staining. Colour conversion was chosen for better visualization of $BAK1^{LRR}$ (red asterisk) co-eluting with $RLP23^{LRR}$ (**d**). Representative results out of three are shown.

defences (Fig. 3e,f and Supplementary Fig. 10). *sobir1* mutants proved entirely insensitive to nlp20 treatment as ethylene formation, ROS production (Fig. 3e,f), callose apposition or MAPK activation (Supplementary Fig. 10a,b) were abolished. Testing nlp peptides from diverse microbial taxa confirmed these findings (Supplementary Fig. 10c). Likewise, nlp20 responsiveness in *bak1-5/bkk1* double mutants was strongly reduced, suggesting that both proteins contribute to RLP23 function (Fig. 3e,f; Supplementary Fig. 10a,b). Residual nlp20 responsiveness in this genotype (Fig. 3e) could be attributed to other, functionally redundant SERK proteins, which is in agreement with ligand-induced complex formation of RLP23 with SERKs1–4 (Fig. 3b) and with reports linking tomato LRR-RPs Cf-4 and Ve1 genetically to SERK1 function[22].

Co-immunoprecipitation assays do not demonstrate physical interaction of proteins in a complex. Ratiometric bimolecular fluorescence complementation assays conducted in transgenic *N. benthamiana* plants verified the proposed direct interaction of RLP23 and SOBIR1 (Fig. 4a). Likewise, *Arabidopsis* protoplasts transiently expressing RLP23–nYFP (yellow fluorescent protein) and SOBIR1–cYFP or SOBIR1–nYFP and RLP23–cYFP constructs, respectively, showed physical interaction of both proteins in the absence of the ligand (Fig. 4b). Recently, a mechanism for ligand-induced complex formation of BAK1 and the LRR-RK PRR FLS2 was proposed in which the ligand "glues" the LRR ectodomains of both proteins[37]. Gel filtration experiments as in[37] were conducted using recombinant RLP23 and BAK1 ectodomains (Fig. 4c). In the absence of nlp20, two separate protein entities migrated without apparent interaction. In contrast, nlp20 caused the RLP23 peak maximum to shift towards a higher molecular weight, which is indicative of nlp20-induced complex formation. Co-elution of RLP23 and BAK1 in the same fractions corroborated this conclusion (Fig. 4d). Altogether, RLP23, SOBIR1 and BAK1 are not only required for nlp20-induced immunity, but appear to be in close physical proximity likely forming a tripartite complex.

RLP23 is required for nlp20-induced resistance. nlp20 (*Pp*NLP) or nlp24 (*Ha*NLP3) treatments rendered *Arabidopsis* Col-0 plants

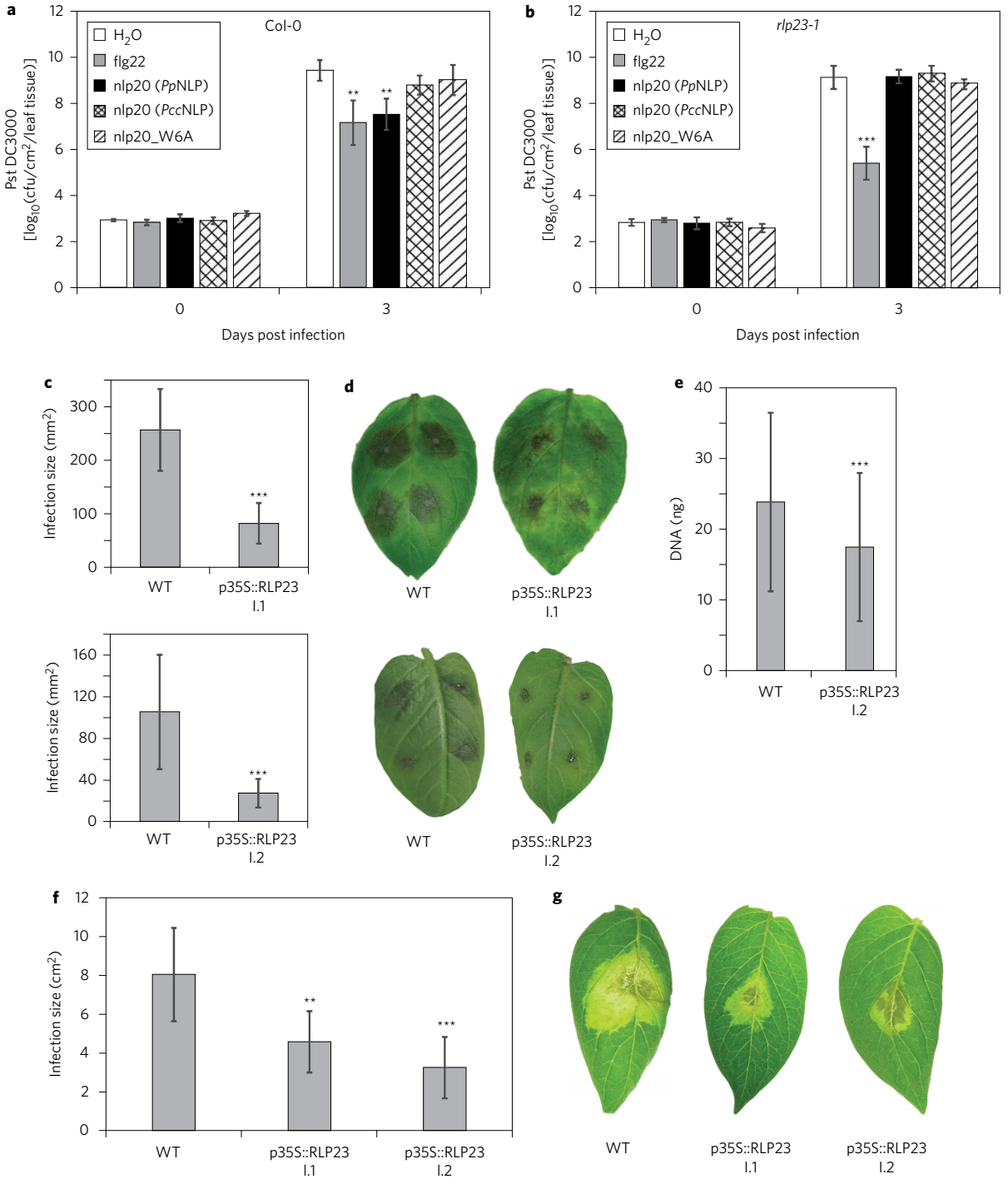

Figure 5 | RLP23-mediated pathogen resistance. a,**b**, Growth of *Pseudomonas syringae* pv. *tomato* on *A. thaliana* Col-0 and *rlp23-1* plants after priming with nlp20 (*Pp*NLP), flg22, and the immunogenically inactive peptides nlp20 (*Pcc*NLP) and nlp20_W6A 24 h before infection. Water infiltration served as a control. **c**,**d**, Disease symptom assessment on wild-type and RLP23-GFP-transgenic *S. tuberosum* lines 4 days post infection with the oomycete *Phytophthora infestans*, strain 88069. **e**, Real-time PCR-based quantification of *P. infestans* growth on infected *S. tuberosum*. **f**,**g**, Disease symptom evaluation of the growth of the fungus *Sclerotinia sclerotiorum* (strain 1980) on RLP23-GFP-transgenic *S. tuberosum* lines 2 days after infection. Experiments were conducted at least three times with similar results. Each data point represents means ± s.d. of $n = 6$ leaves per treatment (**a**,**b**), $n = 24$ leaves per line (**c**, l.1), or $n = 32$ leaves per line (**c**, l.2), $n = 60$ leaves per line (**e**), and $n = 9$ leaves per line (**f**). Asterisks indicate significant differences to water control treatments (**a**,**b**) or WT plants (**c**,**e**,**f**) (**$P < 0.01$, ***$P < 0.001$, Student's *t*-test).

more resistant to subsequent infection with virulent isolates of *Pseudomonas syringae* pv. *tomato* (Fig. 5a), *Botrytis cinerea* or *Hyaloperonospora arabidopsidis*[29,30]. In contrast, pre-treatment with biologically inactive nlp20 derivatives nlp20_W6A or nlp20 from *Pectobacterium carotovorum* NLP (*Pcc*NLP)[29,30] did not affect *Pseudomonas* growth in *Arabidopsis* (Fig. 5a). Notably, nlp20 treatment did not protect *rlp23* mutant genotypes (Fig. 5b and Supplementary Fig. 11a). The deleterious effect was specific to nlp20 since flg22-mediated immunity was not affected in *rlp23* mutants (Fig. 5b and Supplementary Fig. 11a). nlp24 (*Ha*NLP3)

treatment also rendered *Arabidopsis* resistant to the virulent *H. arabidopsidis* isolate Noco2 (Supplementary Fig. 11b). This protective effect was not only detectable in local tissues (Supplementary Fig. 11b), but also systemically (Supplementary Fig. 12). Both, nlp24-induced local and systemic immunity was completely abrogated in *rlp23* and *sobir1* mutants (Supplementary Figs 11b and 12). Altogether, these findings underscore the involvement of RLP23 in nlp-mediated immune activation.

RLP23 expression in potato confers increased resistance to oomycete and fungal pathogens. *Phytophthora infestans*, the potato late blight pathogen and the causal agent of the Irish potato famine in the mid-nineteenth century, harbours a large and fast-evolving family of NLP proteins[38] many of which carry an immunogenic nlp20 motif[29]. To address whether RLP23-mediated sensing of nlp20 would facilitate engineering of enhanced immunity to *P. infestans* infection, transgenic potato lines stably expressing a *p35S::RLP23–GFP* construct were generated. Two lines (I.1, I.2) were tested for their levels of susceptibility to infection with *P. infestans*. Disease-associated lesions were significantly smaller in infected leaves of *RLP23*-expressing lines than those observed in control plants (Fig. 5c,d). Likewise, PCR-based quantification of *P. infestans* colonization revealed statistically significantly reduced pathogen growth in *RLP23*-expressing line I.2 (Fig. 5e). Similarly, disease symptoms caused by the NLP-producing (NPP1 SS1G_11912.3; NPP2 SS1G_03080.3) fungus *Sclerotinia sclerotiorum* strain 1980 were significantly smaller on RLP23-transgenic potato lines (Fig. 5f,g), suggesting that RLP23 confers enhanced protection to these destructive oomycete and fungal pathogens.

Discussion

Employing reverse genetics and exploiting natural variation in nlp20 sensitivity enabled the identification of RLP23 as the *Arabidopsis* nlp20 receptor. Genetic and biochemical evidence supports this notion: (1) *rlp23* mutants lack the ability to mount nlp20-inducible defences, (2) nlp20-insensitive *Arabidopsis* accessions do not produce functional RLP23, (3) ectopic expression of *RLP23*-encoding sequences restores nlp20 recognition in *rlp23* mutants and in insensitive *Arabidopsis* accessions, (4) RLP23 specifically binds nlp20, (5) production of RLP23 in *N. benthamiana*, *S. lycopersicum* and *S. tuberosum* confers nlp20 sensitivity to these nlp20-insensitive species, and (6) wild-type plants, but not *rlp23* mutants are resistant to bacterial and oomycete infection following pre-treatment with nlp20.

LRR-RP receptors carry small cytoplasmic domains without apparent signalling function. It is thus assumed that these proteins require co-receptors for activating intracellular signal transduction[5]. Indeed, the LRR-RP SOBIR1 has been implicated in LRR-RP immune receptor function through serving receptor protein stability and transmembrane signalling[15,16,19,39]. RLP23-dependent nlp20-mediated immune activation also requires SOBIR1, and RLP23 interacts physically *in planta* with SOBIR1 in a ligand-independent manner. RLP23 behaves thus like other immune receptors of the same type, and heteromeric complex formation with SOBIR1 appears to be a common feature of RLP function[5]. *At*SOBIR1 might not be required to stabilize *At*RLP23 as overexpression of *RLP23–GFP* in Col-0 wild-type and *sobir1-12* mutant protoplasts resulted in similar receptor protein levels (data not shown). This is in contrast to tomato SOBIR1, which was reported to stabilize tomato Cf-4 and Ve1 receptors when expressed in *N. benthamiana*[19]. LRR-RP SOBIR1 complexes, formed in a ligand-independent manner, were proposed to constitute bimolecular equivalents of LRR-RKs[5]. This seems to be particularly evident, as LRR-RP function has also been genetically linked to the activity of another co-receptor, BAK1, which is a common co-receptor of LRR-RKs[2,5]. We here show that RLP23-mediated immune activation is dependent on SERK3/BAK1 and possibly other members of the SERK protein family, such as SERK4/BKK1. We also provide evidence that BAK1 is indeed recruited into a pre-formed RLP23-SOBIR1 complex in an nlp20 ligand-dependent manner. We further show, that BAK1 and RLP23 interact physically in a ligand-dependent manner *in vitro*. This finding suggests ligand-mediated stabilization of an LRR-RP receptor/co-receptor complex similar to what was reported for the LRR-RK FLS2 and BAK1 (ref. 37). Altogether, RLP23, SOBIR1 and BAK1 build a signalling-competent array in which all three proteins are in close physical proximity, likely forming a tripartite PRR complex.

Numerous bacterial, oomycete and fungal NLPs carry an immunogenic nlp20 peptide motif[29,30]. Such a broad taxonomic distribution is unknown for any trigger of metazoan or plant immunity. This fact together with a rather plant genus-specific occurrence of nlp20 sensitivity predestined RLP23 as a tool for engineering crop immunity by transfer across genus boundaries. Production of RLP23 in *N. benthamiana*, *S. tuberosum* and *S. lycopersicum* conferred nlp20 sensitivity, suggesting that plants unrelated to *Arabidopsis* could link ectopically expressed PRRs to endogenous immune signalling. More importantly, stable overexpression of RLP23 in potato resulted in significantly enhanced immunity to the major plant pathogens, *P. infestans* and *S. sclerotiorum*. These findings support previous reports on increased resistance to bacterial infections in tomato and wheat plants expressing *Arabidopsis* elongation factor Tu receptor (EFR) (refs 22,40–46). Thus, interfamily transfer of PRRs from model into crop species might constitute a widely applicable strategy for improving immunity. Transfer of individual or stacked PRRs into crops represents a biotechnological alternative to ETI receptor 'stacking' approaches also aiming at engineering crop immunity[47–49]. PRR transfer yields quantitative increases in immunity compared with strong qualitative effects brought about by ETI receptor transfer. Thus, lower selection pressure on pathogen populations by PRR transfer might result in more durable, sustained crop immunity. The nlp20 RLP23 case is paradigmatic for a targeted search for PRRs that recognize broadly distributed patterns from taxonomically unrelated plant pathogens.

Methods

Recombinant protein expression and purification. His-tagged RLP23 and *At*FLS2 LRR domains were expressed using the Bac-to-Bac baculovirus expression system (Invitrogen) in HI-5 cells at 22 °C. Cells (1.8×10^9 cells l^{-1}cultured in the medium from Expression Systems) were infected with 30 ml l^{-1} baculovirus and cultures were harvested 72 h post infection. Proteins were purified by Ni-NTA affinity chromatography (Novagen) and digested with precision protease to remove the carboxy (C)-terminal tag before size exclusion chromatography (HiLoad 200, GE Healthcare) in buffer containing 10 mM Bis-Tris pH 6.0, 100 mM NaCl. The expression and purification of AtFLS2^{LRR} and AtBAK1^{LRR} was as reported[37]. Bacteria harbouring pGEX-6p-1-nlp20 were cultured at 37 °C in LB medium containing 100 mg ml^{-1} ampicillin. The culture was induced by adding 0.2 mM IPTG at OD_{600} = 0.8 and incubated for 3 h at 22 °C. The cell pellets were resuspended in buffer A containing 20 mM Tris HCl (pH 8.0), 150 mM NaCl. After sonication and centrifugation (45 min, 14,000 rpm, 4 °C), the clear supernatant was harvested and applied onto GS4B beads. The column was washed with 10 ml buffer A for three times and eluted with buffer B (20 mM Tris HCl pH 8.0, 50 mM NaCl, 20 mM GSH). The eluate was further loaded onto an ion-exchange column (Source 15Q, GE Healthcare) and then eluted using a linear 100 ml gradient of 0–0.5 M NaCl.

***In vitro* pull-down assay, *in vitro* competition assay and gel filtration assay.** For *in vitro* pull-down and competition assays 30 µg of purified His-tagged RLP23^{LRR} were added to mixtures containing an equal amount of GST-nlp20 and 50 µl of GS4B resin with or without varying concentrations of synthesized nlp20 in buffer containing 10 mM Bis-Tris, pH 6.0, 100 mM NaCl. After incubation on ice for 15–30 min the resin was washed three or four times with 1 ml of buffer. GST–TDIF (Tracheary Element Differentiation Inhibitory Factor or CLE41; primary sequence: HEVPSGPNPISN) and His-tagged FLS2^{LRR} served as negative controls.

Purified RLP23^{LRR} and AtBAK1^{LRR} were incubated for 20 min on ice in the absence or presence of nlp20. Mixtures were subjected to a gel filtration column (HiLoad 200, GE Healthcare) in 10 mM Bis-Tris pH 6.0, 100 mM NaCl. Fractions

from gel filtration and pulled down proteins were subjected to SDS–polyacrylamide gel electrophoresis (PAGE) and detected by Coomassie blue staining.

Immunoprecipitation assays and *in vivo* cross-linking. Leaves of transiently transformed *N. benthamiana* were either harvested directly or 3 min after infiltration of 1 μM nlp20 or SCFE1 (ref. 15). For *in vivo* cross-linking of nlp24-biotin to RLP23 leaves of either *N. benthamiana* or *A. thaliana rlp23–1* expressing 35S::RLP23–GFP, or control plants (*A. thaliana rlp23-1* or *N. benthamiana* expressing 35S::RLP30–GFP), were infiltrated with biotinylated nlp24 (*Pp*NLP) (30 nM in ddH_2O) with or without unlabelled nlp24 (*Pp*NLP) (100 μM) as competitor or with an inactive version of nlp24 (nlp24ΔAIMY, amino acid sequence SWYFPKDSPVTGLGHRHDWE) as competition control. Five minutes after peptide treatment 2 mM EGS (ethylene glycol bis(succinimidyl succinate); initially solved in a small volume of DMSO, further diluted in 25 mM HEPES buffer, pH 7.5) was infiltrated into the same leaves for cross-linking of peptides to the receptor proteins. Thirty minutes after cross-linking, leaf samples were harvested and frozen in liquid nitrogen.

For immunoprecipitations, 300 mg ground leaf material from transiently transformed *N. benthamiana* or 500 mg from *A. thaliana* was used per sample. Membrane proteins were solubilized as described[50] and immuno-adsorbed via the GFP-tag to GFP-Trap beads (ChromoTek, IZB Martinsried, Germany). In the case of BAK1 pull-down experiments, *Arabidopsis rlp23-1/p35S::RLP23–GFP* plants and solubilization and wash buffers containing 20 mM NaCl were used. Protein blots were probed either directly with an Streptavidin-alkaline phosphatase conjugate (Roche) or with antibodies raised against GFP (Torrey Pines Biolabs), HA or Myc-tags (Sigma), BAK1 (Agrisera) or SERK (raised against peptide DIPVNGSFSLFTPISFANTK), followed by staining with secondary antibodies coupled to alkaline phosphatase and CDP-Star (Roche) as substrates. Chemiluminescence was detected using a CCD-camera (Viber Louromat, PeqLAB).

Ratiometric bimolecular fluorescence complementation (rBiFC) and BiFC. For rBiFC, abaxial, transiently transformed *N. benthamiana* leaves were analysed using a Leica SP8 confocal microscope with a 40×/0.75 water-immersion objective. YFP was excited using a 514 nm laser collecting emission between 520–560 nm; the RFP signal was excited using a 561 nm laser with an emission spectrum of 565–620 nm. Mean fluorescence intensity of complemented YFP was ratioed against RFP signal in 30 randomly chosen square sections of ~9500 μm^2, each as described[51]. For BiFC, transformed *A. thaliana* Col-0 protoplasts were investigated as described above on a Leica SP2 confocal microscope with a 20×/0.75 water-immersion objective.

Pathogenicity assays. Four- to 6-week-old *A. thaliana* Col-0 plants were primed 24 h before bacterial or oomycete infection by leaf infiltration of nlp20 *Pp*NLP, nlp24 *Ha*NLP3, flg22 (1 μM peptide solution) or mock treatment, respectively. Infections with *P. syringae* pv. *tomato* DC3000 (*Pst* DC3000), *P. infestans* strain 88069, *S. sclerotiorum* strain 1980 or *H. arabidopsidis* Noco2 and determination of microbial growth rates were as described[15,29,30,52]. For scoring disease development in systemic tissue, conidiophore numbers on non-nlp24-treated leaves were counted at 6 days after inoculation. *P. infestans* DNA from infected potato leaves was extracted as described[53] using 12 mm leaf discs (area 113 mm^2) per sample 4 days after droplet inoculation of 10 μl 5×10^4 zoospores ml^{-1}. DNA quantification was performed by real-time PCR using 1 μl of DNA in 20 μl of buffer including SYBR Green (Thermo Scientific) and an iQ5 iCycler (Bio-Rad). DNA contents were calculated using a calibration curve established for a range of 100 ng to 0.001 ng (spectrophotometric determination, NanoDrop 2000, Thermo Scientific) pure mycelia-derived *P. infestans* DNA. Primers for amplification were chosen based on highly repetitive sequences from the *P. infestans* genome[38] (PiO8-3-3-3 fwd 5′-CAATTCGCCACCTTCTTCGA-3′, PiO8-3-3 rev 5′-GCCTTCCTGCCCTCAAGAAC-3′). Cycling conditions were 10 min 95 °C, 40 cycles 10 s 95 °C, 15 s 59 °C, 20 s 72 °C. Mean values of three technical replicates were used.

Received 20 March 2015; accepted 28 August 2015; published 5 October 2015

References

1. Macho, A. P. & Zipfel, C. Plant PRRs and the activation of innate immune signaling. *Mol. Cell* **54,** 263–272 (2014).
2. Böhm, H., Albert, I., Fan, L., Reinhard, A. & Nürnberger, T. Immune receptor complexes at the plant cell surface. *Curr. Opin. Plant Biol.* **20,** 47–54 (2014).
3. Jones, J. D. & Dangl, J. L. The plant immune system. *Nature* **444,** 323–329 (2006).
4. Nürnberger, T., Brunner, F., Kemmerling, B. & Piater, L. Innate immunity in plants and animals: striking similarities and obvious differences. *Immunol. Rev.* **198,** 249–266 (2004).
5. Gust, A. A. & Felix, G. Receptor like proteins associate with SOBIR1-type of adaptors to form bimolecular receptor kinases. *Curr. Opin. Plant Biol.* **21,** 104–111 (2014).
6. Dou, D. & Zhou, J. M. Phytopathogen effectors subverting host immunity: different foes, similar battleground. *Cell Host Microbe* **12,** 484–495 (2012).
7. Dodds, P. N. & Rathjen, J. P. Plant immunity: towards an integrated view of plant-pathogen interactions. *Nature Rev. Genet.* **11,** 539–548 (2010).
8. Thomma, B. P., Nürnberger, T. & Joosten, M. H. Of PAMPs and effectors: the blurred PTI-ETI dichotomy. *Plant Cell* **23,** 4–15 (2011).
9. Gomez-Gomez, L. & Boller, T. FLS2: an LRR receptor-like kinase involved in the perception of the bacterial elicitor flagellin in *Arabidopsis*. *Mol. Cell* **5,** 1003–1011 (2000).
10. Zipfel, C. *et al.* Perception of the bacterial PAMP EF-Tu by the receptor EFR restricts *Agrobacterium*-mediated transformation. *Cell* **125,** 749–760 (2006).
11. Joosten, M. H., Cozijnsen, T. J. & De Wit, P. J. Host resistance to a fungal tomato pathogen lost by a single base-pair change in an avirulence gene. *Nature* **367,** 384–386 (1994).
12. Thomas, C. M. *et al.* Characterization of the tomato Cf-4 gene for resistance to *Cladosporium fulvum* identifies sequences that determine recognitional specificity in Cf-4 and Cf-9. *Plant Cell* **9,** 2209–2224 (1997).
13. Ron, M. & Avni, A. The receptor for the fungal elicitor ethylene-inducing xylanase is a member of a resistance-like gene family in tomato. *Plant Cell* **16,** 1604–1615 (2004).
14. de Jonge, R. *et al.* Tomato immune receptor Ve1 recognizes effector of multiple fungal pathogens uncovered by genome and RNA sequencing. *Proc. Natl Acad. Sci. USA* **109,** 5110–5115 (2012).
15. Zhang, W. *et al.* Arabidopsis receptor-like protein30 and receptor-like kinase suppressor of BIR1–1/EVERSHED mediate innate immunity to necrotrophic fungi. *Plant Cell* **25,** 4227–4241 (2013).
16. Zhang, L. *et al.* Fungal endopolygalacturonases are recognized as microbe-associated molecular patterns by the *Arabidopsis* receptor-like protein RESPONSIVENESS TO BOTRYTIS POLYGALACTURONASES1. *Plant Physiol.* **164,** 352–364 (2014).
17. Jehle, A. K. *et al.* The receptor-like protein ReMAX of *Arabidopsis* detects the microbe-associated molecular pattern eMax from Xanthomonas. *Plant Cell* **25,** 2330–2340 (2013).
18. Du, J. *et al.* Elicitin recognition confers enhanced resistance to *Phytophthora infestans* in potato. *Nature Plants* doi:10.1038/nplants.2015.34 (2015).
19. Liebrand, T. W. *et al.* Receptor-like kinase SOBIR1/EVR interacts with receptor-like proteins in plant immunity against fungal infection. *Proc. Natl Acad. Sci. USA* **110,** 10010–10015 (2013).
20. Chinchilla, D., Shan, L., He, P., de Vries, S. & Kemmerling, B. One for all: the receptor-associated kinase BAK1. *Trends Plant Sci.* **14,** 535–541 (2009).
21. Bar, M., Sharfman, M., Ron, M. & Avni, A. BAK1 is required for the attenuation of ethylene-inducing xylanase (Eix)-induced defense responses by the decoy receptor LeEix1. *Plant J.* **63,** 791–800 (2010).
22. Fradin, E. F. *et al.* Interfamily transfer of tomato Ve1 mediates Verticillium resistance in Arabidopsis. *Plant Physiol.* **156,** 2255–2265 (2011).
23. Gijzen, M. & Nürnberger, T. Nep1-like proteins from plant pathogens: recruitment and diversification of the NPP1 domain across taxa. *Phytochemistry* **67,** 1800–1807 (2006).
24. Oome, S. & Van den Ackerveken, G. Comparative and functional analysis of the widely occurring family of nep1-like proteins. *Mol. Plant Microbe Interact.* **27,** 1081–1094 (2014).
25. Qutob, D. *et al.* Phytotoxicity and innate immune responses induced by Nep1-like proteins. *Plant Cell* **18,** 3721–3744 (2006).
26. Cabral, A. *et al.* Nontoxic Nep1-like proteins of the downy mildew pathogen Hyaloperonospora arabidopsidis repression of necrosis-inducing activity by a surface-exposed region. *Mol. Plant Microbe Interact.* **25,** 697–708 (2012).
27. Dong, S. *et al.* The NLP toxin family in Phytophthora sojae includes rapidly evolving groups that lack necrosis-inducing activity. *Mol. Plant Microbe Interact.* **25,** 896–909 (2012).
28. Santhanam, P. *et al.* Evidence for functional diversification within a fungal NEP1-like protein family. *Mol. Plant Microbe Interact.* **26,** 278–286 (2013).
29. Böhm, H. *et al.* A conserved peptide pattern from a widespread microbial virulence factor triggers pattern-induced immunity in *Arabidopsis*. *PLoS Pathog.* **10,** e1004491 (2014).
30. Oome, S. *et al.* Nep1-like proteins from three kingdoms of life act as a microbe-associated molecular pattern in *Arabidopsis*. *Proc. Natl Acad. Sci. USA* **111,** 16955–16960 (2014).
31. Postel, S. *et al.* The multifunctional leucine-rich repeat receptor kinase BAK1 is implicated in *Arabidopsis* development and immunity. *Eur. J. Cell Biol.* **89,** 169–174 (2010).
32. Wang, G. *et al.* A genome-wide functional investigation into the roles of receptor-like proteins in *Arabidopsis*. *Plant Physiol.* **147,** 503–5017 (2008).
33. Jeworutzki, E. *et al.* Early signaling through the *Arabidopsis* pattern recognition receptors FLS2 and EFR involves Ca-associated opening of plasma membrane anion channels. *Plant J.* **62,** 367–378 (2010).
34. Krol, E. *et al.* Perception of the *Arabidopsis* danger signal peptide 1 involves the pattern recognition receptor AtPEPR1 and its close homologue AtPEPR2. *J. Biol. Chem.* **285,** 13471–13479 (2010).
35. Bi, G. *et al. Arabidopsis thaliana* receptor-like protein AtRLP23 associates with the receptor-like kinase AtSOBIR1. *Plant Signal Behav.* **9,** e27937 (2014).

36. Santiago, J., Henzler, C. & Hothorn, M. Molecular mechanism for plant steroid receptor activation by somatic embryogenesis co-receptor kinases. *Science* **341,** 889–892 (2013).
37. Sun, Y. *et al.* Structural basis for flg22-induced activation of the *Arabidopsis* FLS2-BAK1 immune complex. *Science* **342,** 624–628 (2013).
38. Haas, B. J. *et al.* Genome sequence and analysis of the Irish potato famine pathogen *Phytophthora infestans*. *Nature* **461,** 393–398 (2009).
39. Jehle, A. K., Fürst, U., Lipschis, M., Albert, M. & Felix, G. Perception of the novel MAMP eMax from different *Xanthomonas* species requires the *Arabidopsis* receptor-like protein ReMAX and the receptor kinase SOBIR. *Plant. Signal Behav.* **8,** pii: e27408 (2013).
40. Lacombe, S. *et al.* Interfamily transfer of a plant pattern-recognition receptor confers broad-spectrum bacterial resistance. *Nature Biotechnol.* **28,** 365–369 (2010).
41. Schoonbeek, H. J. *et al.* Arabidopsis EF-Tu receptor enhances bacterial disease resistance in transgenic wheat. *New Phytol.* **206,** 606–613 (2015).
42. Afroz, A. *et al.* Enhanced resistance against bacterial wilt in transgenic tomato (Lycopersicon esculentum) lines expressing the Xa21 gene. *Plant Cell Tiss. Organ Cult.* **104,** 227–237 (2010).
43. Holton, N., Nekrasov, V., Ronald, P. C. & Zipfel, C. The phylogenetically-related pattern recognition receptors EFR and XA21 recruit similar immune signaling components in monocots and dicots. *PLoS Pathog.* **11,** e1004602 (2015).
44. Mendes, B. M. J. *et al.* Reduction in susceptibility to *Xanthomonas axonopodis* pv. *citri* in transgenic Citrus sinensis expressing the rice Xa21 gene. *Plant Pathol.* **59,** 68–75 (2010).
45. Schwessinger, B. *et al.* Transgenic expression of the dicotyledonous pattern recognition receptor EFR in rice leads to ligand-dependent activation of defense responses. *PLoS Pathog.* **11,** e1004809 (2015).
46. Tripathi, J. N., Lorenzen, J., Bahar, O., Ronald, P. & Tripathi, L. Transgenic expression of the rice Xa21 pattern-recognition receptor in banana (Musa sp.) confers resistance to *Xanthomonas campestris* pv. *muscearum*. *Plant Biotechnol. J.* **12,** 663–673 (2014).
47. Dangl, J. L., Horvath, D. M. & Staskawicz, B. J. Pivoting the plant immune system from dissection to deployment. *Science* **341,** 746–751 (2013).
48. Gust, A. A., Brunner, F. & Nürnberger, T. Biotechnological concepts for improving plant innate immunity. *Curr. Opin. Biotechnol.* **21,** 204–210 (2010).
49. Monaghan, J. & Zipfel, C. Plant pattern recognition receptor complexes at the plasma membrane. *Curr. Opin. Plant Biol.* **15,** 349–357 (2012).
50. Chinchilla, D. *et al.* A flagellin-induced complex of the receptor FLS2 and BAK1 initiates plant defence. *Nature* **448,** 497–500 (2007).
51. Grefen, C. & Blatt, M. R. A 2in1 cloning system enables ratiometric bimolecular fluorescence complementation (rBiFC). *BioTechniques* **53,** 311–314 (2012).
52. McLellan, H. *et al.* An RxLR effector from *Phytophthora infestans* prevents re-localisation of two plant NAC transcription factors from the endoplasmic reticulum to the nucleus. *PLoS Pathog.* **9,** e1003670 (2013).
53. Llorente, B. *et al.* A quantitative real-time PCR method for in planta monitoring of Phytophthora infestans growth. *Lett. Appl. Microbiol.* **51,** 603–610 (2010).

Acknowledgements

Research in the laboratory of T.N. was funded by DFG grant Nu 70/9, funds of the University of Tübingen and SFB1101. Research in the G.V.d.A. laboratory was partly financed by a 'more with less' grant of the Netherlands Organization for Scientific Research. We are grateful to C. Oecking for critical discussions, to K. Berendzen for technical advice and to D. Chinchilla and J. Felix for providing an anti-SERK-antibody.

Author contributions

T.N., G.V.d.A., J.C., R.H., I.A., H.B., M.A., J.I., S.O., T.M.R., C.G., A.A.G. and E.K. conceived and designed the experiments; I.A., H.B., M.A., C.F., J.I., N.W., C.G., T.M.R., H.Z. and E.K. conducted experiments and analysed data; C.B. produced transgenic plants; and I.A., H.B. and T.N. wrote the manuscript. All authors discussed the results and commented on the manuscript.

Additional information

Supplementary information is available online. Reprints and permissions information is available online at www.nature.com/reprints. Correspondence and requests for materials should be addressed to T.N.

Competing interests

The authors declare no competing financial interests.

nature plants

SUPPLEMENTARY INFORMATION

DOI: 10.1038/NPLANTS.2015.140

An RLP23–SOBIR1–BAK1 complex mediates NLP-triggered immunity

Supplemental methods

Peptides. Synthetic peptides including nlp24:bio purchased from Genscript Inc. were prepared as 10 mM stock solutions in 100 % DMSO, and diluted in water prior to use. DMSO concentrations corresponding to those in peptide solutions used in this study did not trigger plant responses[1]. nlp20 peptides used herein were deduced from *Phytophthora parasitica* *Pp*NLP[1] if not stated otherwise.

Plant materials and growth conditions. *Arabidopsis* plants were grown in soil (22 °C, 8 h light/16 h dark diurnal cycle) and used at an age of 4-6 weeks. Plants used for infections with *P. syringae* or *P. infestans* were grown under translucent cover. *Nicotiana benthamiana* plants were grown in the greenhouse (16 h light, 22 °C/8 h dark, 18 °C) and used at an age of 4-5 weeks. For stable transformation, *N. benthamiana* (7-8 weeks old, 13 h light/11 h dark at 23 °C), *Solanum tuberosum* var. Désirée (3-4 weeks old, 14 h light/10 h dark, 23 °C) and *Solanum lycopersicum* (2 weeks old, 14 h light/10 dark, 23 °C) were grown in sterile culture on MS medium containing 2 % sucrose. Transgenic *N. benthamiana*, *S. tuberosum* and *S. lycopersicum* were grown in soil in the greenhouse under long day conditions (16 h light/8 h dark, 23 °C).

Genotyping of *Arabidopsis rlp23* mutant lines. PCR on genomic DNA was performed using the Phire Plant Direct PCR Kit (Life Technologies) and primers RLP23for, RLP23rev, RLP23mid_rev (mr) (TGAGCAGTTTACAAAAGACC), SALK_LB (ctttgacgttggagtccac) and GABI_Kat_LB (CCCATTTGGACGTGAATGTAGACAC). Transcript levels in WT and mutant plants were detected by PCR on cDNA with Taq Polymerase (Life Technologies) using the Primers RLP23for and RLP23rev as well as EF-1alpha_for (TCACATCAACATTGTGGTCATTGG) and EF-1alpha_rev (TTGATCTGGTCAAGAGCCTACAG) as control.

DOI: 10.1038/NPLANTS.2015.140

Plant responses. Ethylene production was performed as described[2]. Leaf pieces were incubated in 20 mM MES buffer, pH 5.7. For ROS burst measurements leaves were cut in pieces (2x3 mm size) and floated on H_2O for 12 hrs in petri dishes. Two leaf pieces/well of a white 96-well plate (Greiner BioOne) were incubated in 100 µl 20 µM L-012, 0.5 µg/ml peroxidase solution. Background luminescence was recorded for 10 min in a 96-well luminometer, (Mithras LB 940, Berthold Technologies) before elicitation or control treatments. Measurements were performed for 30 min with signal integration times of 1 s in 1 min intervals. For MAPK activity assays, infiltrated plant material was harvested after 15 min and frozen in liquid nitrogen prior to protein extraction in 20 mM Tris-HCl pH 7.5, 150 mM NaCl, 1 mM EDTA, 1 % Triton X-100, 0.1 % SDS, 5 mM DTT, Complete Protease Inhibitor Mini, EDTA-free (Roche, Mannheim), PhosStop Phosphatase Inhibitor Cocktail (Roche, Mannheim). After pelleting cell debris (10 min, 16000 g, 4 °C), the supernatant (30 µg protein) was separated on 10 % SDS-PAGE, transferred to nitrocellulose, and activated MAPK6, 3 and 4 were detected by protein blotting using the rabbit anti-phospho-p44/42-MAPK antibody (Cell Signalling Technology, The Netherlands). To visualize callose apposition, leaves were treated as described[1] and harvested 24 hours after infiltration of a peptide solution. Quantification of callose was performed by counting selected pixels and calculated in % relative to the respective image section of the leaf surface. Pictures were analysed using the Photoshop CS6 Magic tool, hereby removing background and leaf-veins within a certain colour range. (use: white, mode: normal, opacity: 100%). Membrane potential measurements were performed on detached leaves that were glued to the base of a patch-clamp chamber (adaxial site), peeled off (abaxial epidermis) and left for recovery overnight in standard solution (0.1 mM KCl, 1 mM $CaCl_2$, 5 mM MES pH 5.5). During experiments, exposed tissue was constantly perfused with standard solution (2 ml/min), and elicitors were applied for 1-2 min unless stated otherwise. For impalements, microelectrodes of borosilicate glass capillaries with filament (Hilgenberg, Malsfeld, Germany) pulled on a horizontal laser puller (P2000, Sutter Instruments Co, Novato, CA, USA) were filled with 300 mM KCl, and

connected by an Ag/AgCl half-cell to a headstage (1 GΩ, HS-2A, Axon Inst., Union City, CA, USA). Tip-resistance was approximately 20-50 MΩ, whereas the input resistance of the headstage was 10^{13} Ω. The reference electrode was also filled with 300 mM KCl. Cells were impaled using an electronic micromanipulator (NC-30, Kleindiek Nanotechnik, Germany). Recordings were amplified with an IPA-2 amplifier (Applicable Electronics, Inc., Forestdale, MA, USA) and stored using WinEDR software on a Windows Electrophysiology Disk Recorder.

LC-MS/MS analysis. Leaf material (3 g) from *A. thaliana* Col-0 plants or *rlp23*-1 plants overexpressing RLP23:GFP was harvested directly or 10 min after infiltration of 100 nM nlp20. Membrane proteins were solubilized and immuno-adsorbed via the GFP-tag to GFP-Trap® beads (ChromoTek, IZB Martinsried, Germany). Samples were resuspended in SDS-loading buffer, applied to an SDS-PAGE and excised from the stacking gel. Following a tryptic digestion, LC-MS/MS analysis was performed on a Proxeon Easy-nLC coupled to an LTQ Orbitrap Elite mass spectrometer (method: 130 min Top15HCD). Processing of the data was conducted using MaxQuant software suite v.1.2.2.9[3]. Using the Andromeda search engine[4], spectra were compared to an *Arabidopsis thaliana* database and a database comprising protein sequences of interest. Raw data processing was performed with 1 % false discovery rate setting. PEP scores <0.2 were considered to identify peptides derived from biologically significant interacting proteins.

RNA isolation and cloning of constructs. RNA was isolated from *A. thaliana* Col-0 using the RNeasy Plant MiniKit (Qiagen) and cDNA synthesis was performed using RevertAidTM MuLV reverse transcriptase (Thermo Scientific). PCR assays were performed with Pfu DNA Polymerase (Thermo Scientific). *RLP23*, *SOBIR1* and *BAK1* coding sequences or coding sequences together with the native promoter were amplified with Pfu DNA Polymerase (Thermo Scientific), cloned into pCR8-Topo vector (Gateway vector; Invitrogen) using primers PromRLP23for (ATACATGTTCACTCATCTTTCC), RLP23for

DOI: 10.1038/NPLANTS.2015.140

(ATGTCAAAGGCGCTTTTGCATTTGC), RLP23revW/oStop (ACGCTTTCTGCGTTTATTCAGACC), SOBIR1for (ATGGCTGTTCCCACGGGAAGC), SOBIR1revW/oStop (GTGCTTGATCTGGGACAACATGG), BAK1for (ATGGAACGAAGATTAATGATCC), BAK1revW/oStop (TCTTGGACCCGAGGGGTATTCG) and recombined to pB7FWG2.0 (Plant Systems Biology, VIB, University of Ghent) for C-terminal GFP fusion, to pGWB14 for C-terminal HA fusion to pGWB17 for C-terminal Myc fusion[5], pUBC-nYFP-DEST and pUBC-cYFP-DEST for C-terminal n- or cYFP fusions. For rBIFC constructs RLP23, SOBIR1, CERK1 and EFR were amplified using the primers AttB3-RLP23-S (ggggacaactttgtataataaagttgtaATGTCAAAGGCGCTTTTGC), AttB2-RLP23-AS (ggggaccactttgtacaagaaagctgggtGACGCTTTCTGCGTTTATTCAG), AttB1-SOBIR-S (ggggacaagtttgtacaaaaaagcaggctTAATGGCTGTTCCCACGGGA), AttB4-SOBIR-AS (ggggacaactttgtatagaaaagttgggttGTGCTTGATCTGGGACAACATG), AttB3-EFR-S (ggggacaactttgtataataaagttgtaATGAAGCTGTCCTTTTCACTTG), AttB2-EFR-AS (ggggaccactttgtacaagaaagctgggttCATAGTATGCATGTCCGTATT), AttB1-CERK1-S (ggggacaagtttgtacaaaaaagcaggcttaATGAAGCTAAAGATTTCTCTAA), AttB4-CERK1-AS (ggggacaactttgtatagaaaagttgggttCCGGCCGGACATAAGACTGAC) and recombined into the plasmid pBiFCt-2in1-CC.

The ectodomains of RLP23 (RLP23^{LRR}, residues 1-832) and *At*FLS2 (FLS2^{LRR}, residues 25-800) carrying C-terminal 6xHis-tags and nlp20 carrying N-terminal GST-tag were generated by standard PCR strategies and cloned into the expression vector pFastBacTM1 (Invitrogen) or pGEX-6P-1 (GE life sciences). Their identities were confirmed by sequencing. Primers used were RLP23-BamHI (ggaattggatccatgtcaaaggcgcttttg), RLP23-832-SalI (gaaattgtcgacgtcttcttgcttttg), NLP20-BamHI (ggaattggatccgctatcatgtactcgtgg), NLP20-XhoI (gaaattctcgagctagcgatgccccagtccagt), BAK1-BamHI (ggaattggatccatggaacgaagattaatg) and BAK1-220-XhoI (gaaattctcgagATGATGATGATGATGATGgtttgagagatccag).

Plant and protoplast transformation. *A. tumefaciens* GV3101 harbouring the gene constructs to be expressed were grown for 48 h in LB medium, collected by centrifugation,

and adjusted to OD_{600} of 0.1 in induction medium (10 mM $MgCl_2$, 150 µM acetosyringone). For transient gene expression, bacteria were pressure-infiltrated into *N. benthamiana* leaves after incubation at room temperature for 1 h. Leaves were used for ethylene measurements, protein expression analysis or immunoprecipitation at 48 hours after infiltration. For stable transformation, *A. tumefaciens* Gv3101 carrying the desired constructs were grown in LB medium with appropriate antibiotics. For *Arabidopsis* transformation, bacteria cells were harvested and resuspended in 5 % (w/v) Sucrose, 10 mM $MgSO_4$, 0.01 % Silwet and sprayed on buds of 6-8 week old Col-0 *rlp23-1* and *rlp23-2* or accessions Bor-4 and Kyoto. The T1 generation was selected on 0.2 % BASTA. For *Nicotiana benthamiana*, *S. lycopersicum* and *S. tuberosum* transformation, cells were resuspended in 10 mM $MgCl_2$. *N. benthamiana* leaf pieces were incubated in suspension for 3 minutes, subsequently transferred to MS medium with 2 % sucrose, and incubated for 48 hrs in the dark. Transgenic calli were selected on MS medium with BASTA. *S. tuberosum* leaf pieces were floated in liquid 2x MS medium containing *A. tumefaciens* for 3 days in the dark at room temperature and subsequently transferred to callus induction medium for 1 week and to selection medium with BASTA. *S. lycopersicum* cotyledons were incubated in *A. tumefaciens* suspension for 2 days in the dark at room temperature and transferred to selection medium containing BASTA. Transgenic plants selected in sterile culture were transferred to soil and grown in the greenhouse under long day conditions. Protoplasts from *Arabidopsis* Col-0 plants were isolated and transformed as described[6].

1 Böhm, H. *et al.* A conserved peptide pattern from a widespread microbial virulence factor triggers pattern-induced immunity in Arabidopsis. *PLOS Pathogens* **10**, e1004491 (2014).

2 Felix, G., Duran, J. D., Volko, S. & Boller, T. Plants have a sensitive perception system for the most conserved domain of bacterial flagellin. *Plant J* **18**, 265-276 (1999).

DOI: 10.1038/NPLANTS.2015.140

3 Cox, J. & Mann, M. MaxQuant enables high peptide identification rates, individualized p.p.b.-range mass accuracies and proteome-wide protein quantification. *Nature Biotechnol* **26**, 1367-1372 (2008).

4 Cox, J. *et al.* Andromeda: a peptide search engine integrated into the MaxQuant environment. *J Proteome Res* **10**, 1794-1805 (2011).

5 Nakagawa, T. *et al.* Development of series of gateway binary vectors, pGWBs, for realizing efficient construction of fusion genes for plant transformation. *J Biosci Bioeng* **104**, 34-41 (2007).

6 Yoo, S. D., Cho, Y. H. & Sheen, J. Arabidopsis mesophyll protoplasts: a versatile cell system for transient gene expression analysis. *Nature Protoc* **2**, 1565-1572, doi:10.1038/nprot.2007.199 (2007).

Fig. S1

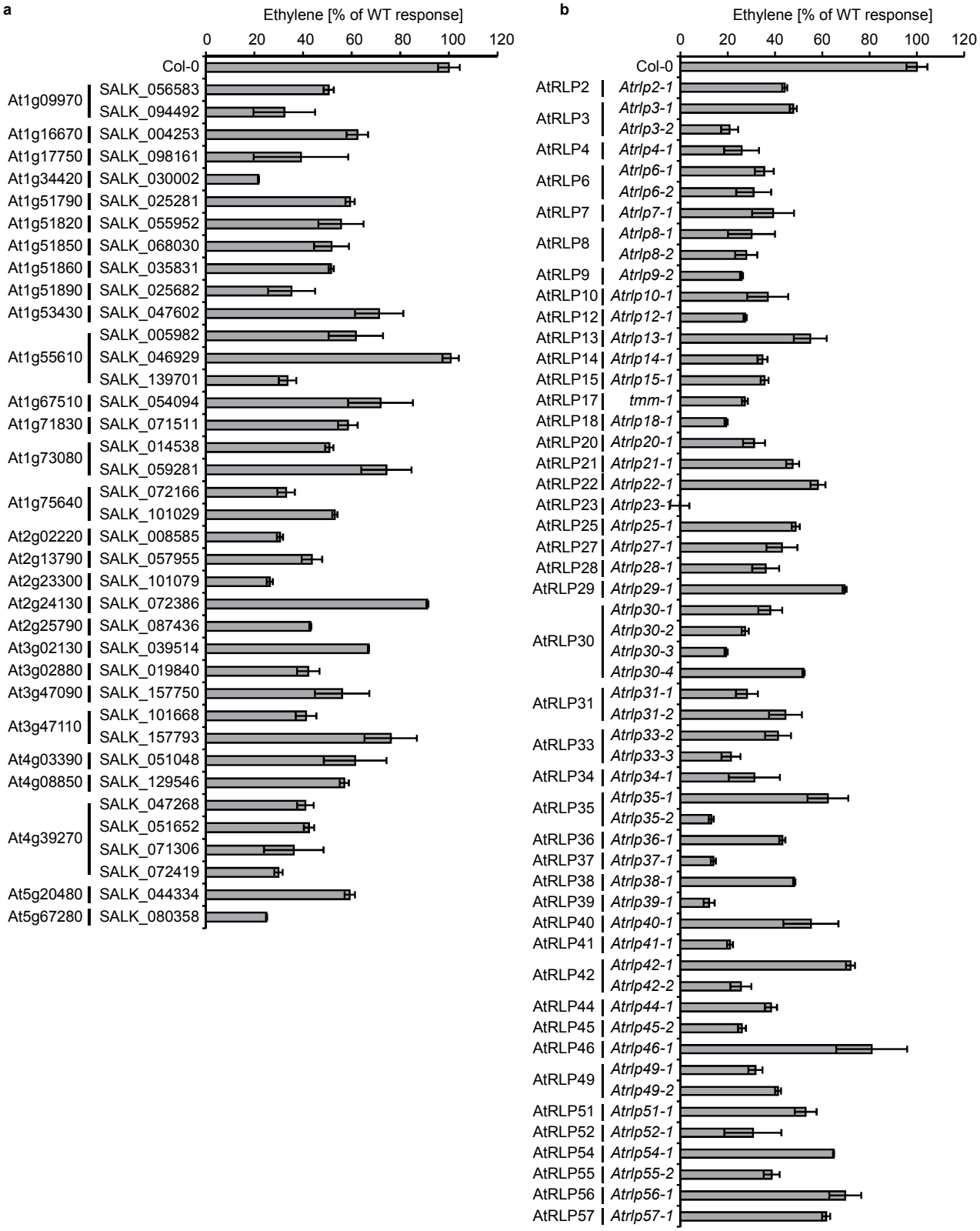
a
Ethylene [% of WT response]
0 20 40 60 80 100 120
Col-0
At1g09970 SALK_056583
SALK_094492
At1g16670 SALK_004253
At1g17750 SALK_098161
At1g34420 SALK_030002
At1g51790 SALK_025281
At1g51820 SALK_055952
At1g51850 SALK_068030
At1g51860 SALK_035831
At1g51890 SALK_025682
At1g53430 SALK_047602
At1g55610 SALK_005982
SALK_046929
SALK_139701
At1g67510 SALK_054094
At1g71830 SALK_071511
At1g73080 SALK_014538
SALK_059281
At1g75640 SALK_072166
SALK_101029
At2g02220 SALK_008585
At2g13790 SALK_057955
At2g23300 SALK_101079
At2g24130 SALK_072386
At2g25790 SALK_087436
At3g02130 SALK_039514
At3g02880 SALK_019840
At3g47090 SALK_157750
At3g47110 SALK_101668
SALK_157793
At4g03390 SALK_051048
At4g08850 SALK_129546
At4g39270 SALK_047268
SALK_051652
SALK_071306
SALK_072419
At5g20480 SALK_044334
At5g67280 SALK_080358
b
Ethylene [% of WT response]
0 20 40 60 80 100 120
Col-0
AtRLP2 Atrlp2-1
AtRLP3 Atrlp3-1
Atrlp3-2
AtRLP4 Atrlp4-1
AtRLP6 Atrlp6-1
Atrlp6-2
AtRLP7 Atrlp7-1
AtRLP8 Atrlp8-1
Atrlp8-2
AtRLP9 Atrlp9-2
AtRLP10 Atrlp10-1
AtRLP12 Atrlp12-1
AtRLP13 Atrlp13-1
AtRLP14 Atrlp14-1
AtRLP15 Atrlp15-1
AtRLP17 tmm-1
AtRLP18 Atrlp18-1
AtRLP20 Atrlp20-1
AtRLP21 Atrlp21-1
AtRLP22 Atrlp22-1
AtRLP23 Atrlp23-1
AtRLP25 Atrlp25-1
AtRLP27 Atrlp27-1
AtRLP28 Atrlp28-1
AtRLP29 Atrlp29-1
AtRLP30 Atrlp30-1
Atrlp30-2
Atrlp30-3
Atrlp30-4
AtRLP31 Atrlp31-1
Atrlp31-2
AtRLP33 Atrlp33-2
Atrlp33-3
AtRLP34 Atrlp34-1
AtRLP35 Atrlp35-1
Atrlp35-2
AtRLP36 Atrlp36-1
AtRLP37 Atrlp37-1
AtRLP38 Atrlp38-1
AtRLP39 Atrlp39-1
AtRLP40 Atrlp40-1
AtRLP41 Atrlp41-1
AtRLP42 Atrlp42-1
Atrlp42-2
AtRLP44 Atrlp44-1
AtRLP45 Atrlp45-2
AtRLP46 Atrlp46-1
AtRLP49 Atrlp49-1
Atrlp49-2
AtRLP51 Atrlp51-1
AtRLP52 Atrlp52-1
AtRLP54 Atrlp54-1
AtRLP55 Atrlp55-2
AtRLP56 Atrlp56-1
AtRLP57 Atrlp57-1

DOI: 10.1038/NPLANTS.2015.140

Supplementary Fig. 1: RLK and RLP T-DNA mutants tested for nlp20 sensitivity. a, Ethylene accumulation of 38 T-DNA insertion mutants for 29 RLKs upon nlp20 treatment (1 μM). **b**, Ethylene accumulation of 55 T-DNA insertion mutants for 44 RLPs upon nlp20 (1 μM) treatment. Results are shown as percentage of responses determined in Col-0. Bars represent means of 2 replicates ± standard deviation.

Fig. S2

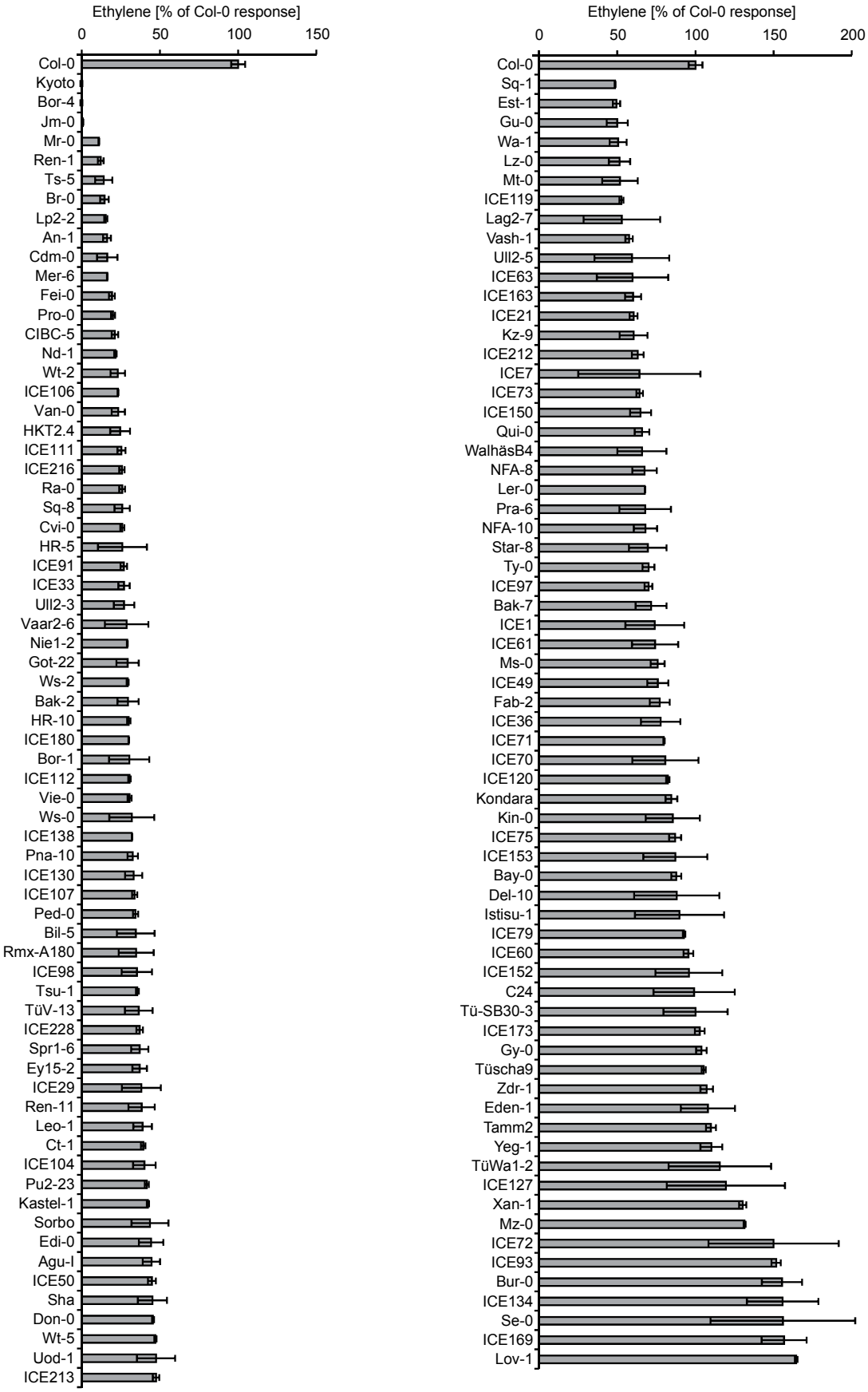
Ethylene [% of Col-0 response]
0
50
100
150
Col-0
Kyoto
Bor-4
Jm-0
Mr-0
Ren-1
Ts-5
Br-0
Lp2-2
An-1
Cdm-0
Mer-6
Fei-0
Pro-0
CIBC-5
Nd-1
Wt-2
ICE106
Van-0
HKT2.4
ICE111
ICE216
Ra-0
Sq-8
Cvi-0
HR-5
ICE91
ICE33
Ull2-3
Vaar2-6
Nie1-2
Got-22
Ws-2
Bak-2
HR-10
ICE180
Bor-1
ICE112
Vie-0
Ws-0
ICE138
Pna-10
ICE130
ICE107
Ped-0
Bil-5
Rmx-A180
ICE98
Tsu-1
TüV-13
ICE228
Spr1-6
Ey15-2
ICE29
Ren-11
Leo-1
Ct-1
ICE104
Pu2-23
Kastel-1
Sorbo
Edi-0
Agu-I
ICE50
Sha
Don-0
Wt-5
Uod-1
ICE213
Ethylene [% of Col-0 response]
0
50
100
150
200
Col-0
Sq-1
Est-1
Gu-0
Wa-1
Lz-0
Mt-0
ICE119
Lag2-7
Vash-1
Ull2-5
ICE63
ICE163
ICE21
Kz-9
ICE212
ICE7
ICE73
ICE150
Qui-0
WalhäsB4
NFA-8
Ler-0
Pra-6
NFA-10
Star-8
Ty-0
ICE97
Bak-7
ICE1
ICE61
Ms-0
ICE49
Fab-2
ICE36
ICE71
ICE70
ICE120
Kondara
Kin-0
ICE75
ICE153
Bay-0
Del-10
Istisu-1
ICE79
ICE60
ICE152
C24
Tü-SB30-3
ICE173
Gy-0
Tüscha9
Zdr-1
Eden-1
Tamm2
Yeg-1
TüWa1-2
ICE127
Xan-1
Mz-0
ICE72
ICE93
Bur-0
ICE134
Se-0
ICE169
Lov-1

DOI: 10.1038/NPLANTS.2015.140

Supplementary Fig. 2: *Arabidopsis thaliana* accessions tested for nlp20 sensitivity. 135 *Arabidopsis thaliana* ecotypes were tested for ethylene accumulation upon nlp20 treatment (1 μM). Results are shown as percentage of responses determined in Col-0. Bars represent means of 2 replicates ± standard deviation.

Fig. S3

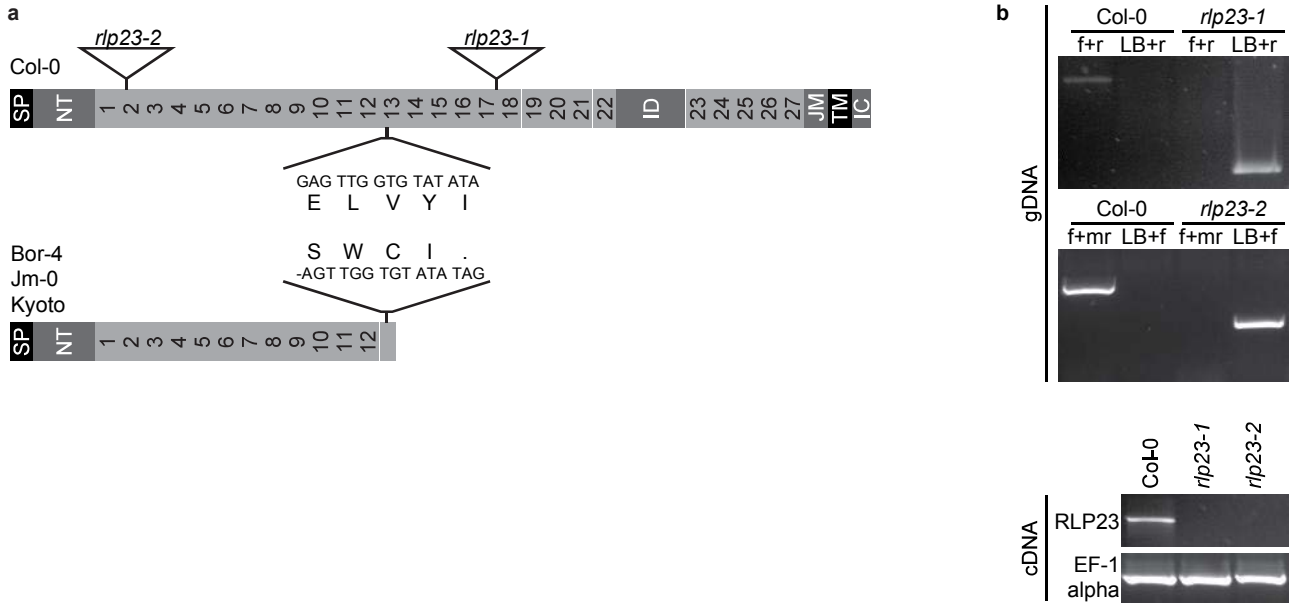
a
rlp23-2
rlp23-1
Col-0
SP NT 1 2 3 4 5 6 7 8 9 10 11 12 13 14 15 16 17 18 19 20 21 22 ID 23 24 25 26 27 JM TM IC
GAG TTG GTG TAT ATA
E L V Y I
Bor-4
Jm-0
Kyoto
S W C I .
-AGT TGG TGT ATA TAG
SP NT 1 2 3 4 5 6 7 8 9 10 11 12
b
Col-0
rlp23-1
f+r LB+r f+r LB+r
gDNA
Col-0
rlp23-2
f+mr LB+f f+mr LB+f
Col-0
rlp23-1
rlp23-2
cDNA
RLP23
EF-1 alpha

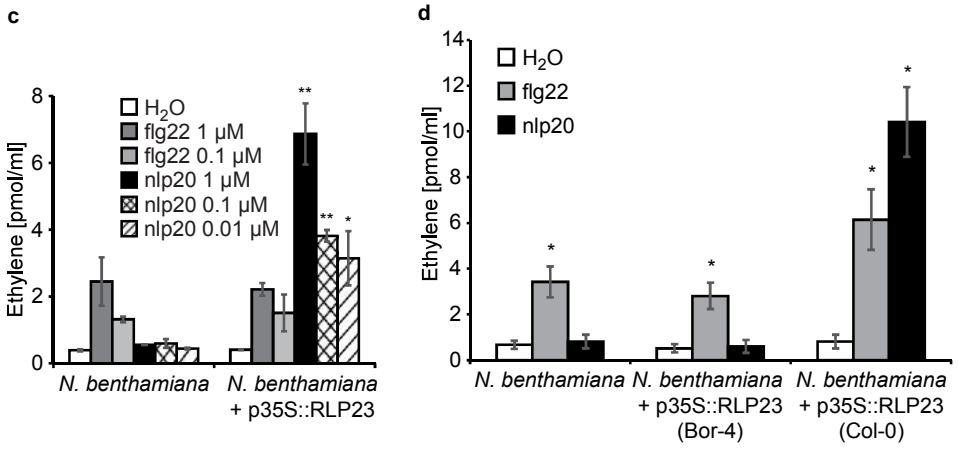
c
Ethylene [pmol/ml]
H2O
flg22 1 µM
flg22 0.1 µM
nlp20 1 µM
nlp20 0.1 µM
nlp20 0.01 µM
N. benthamiana
N. benthamiana + p35S::RLP23
d
Ethylene [pmol/ml]
H2O
flg22
nlp20
N. benthamiana
N. benthamiana + p35S::RLP23 (Bor-4)
N. benthamiana + p35S::RLP23 (Col-0)

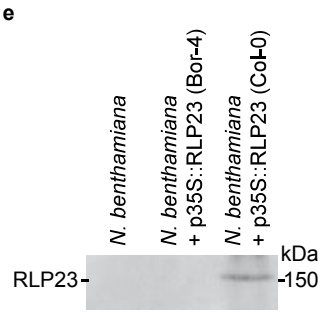
e
N. benthamiana
N. benthamiana + p35S::RLP23 (Bor-4)
N. benthamiana + p35S::RLP23 (Col-0)
kDa
RLP23
150

DOI: 10.1038/NPLANTS.2015.140

Supplementary Fig. 3: RLP23 confers nlp20 sensitivity. a, Schematic representation of the RLP23 protein structure in accessions Col-0, Bor-4, Jm-0, Kyoto, and genotypes *rlp23-1* and *rlp23-2*. SP: signal peptide; NT: N-terminal domain; ID: island domain; JM: juxtamembrane domain; LRR: leucine-rich repeat; TM: transmembrane domain; IC: intracellular domain. **b**, PCR-based genotyping of *rlp23-1* and *rlp23-2* mutants on genomic DNA (gDNA) with gene- (f+r, f+mr) and insertion- specific primer pairs (LB+r, LB+f). PCR on cDNA of the same plants confirmed the absence of full-length transcript, in contrast to amplification of EF-1α as control **c**, **d**, Ethylene accumulation in nlp20-treated (1 μM) *N. benthamiana* plants transiently expressing RLP23:GFP (Col-0) (**c, d**) and RLP23:GFP (Bor-4) alleles (**d**). Water and flagellin (1 μM) were used as control. Bars represent means ± SD of three replicates. Asterisks indicate significant differences to water control treatments (* = $P<0.05$, ** = $P<0.01$, *** = $P<0.001$, Students t-test). **e**, Protein blot of extracts from *N. benthamiana* plants used in **c**, **d**. Protein accumulation in *p35S::RLP23:GFP (Bor-4)* plants is not detectable due to a frameshift mutation in this *RLP23* allele.

Fig. S4

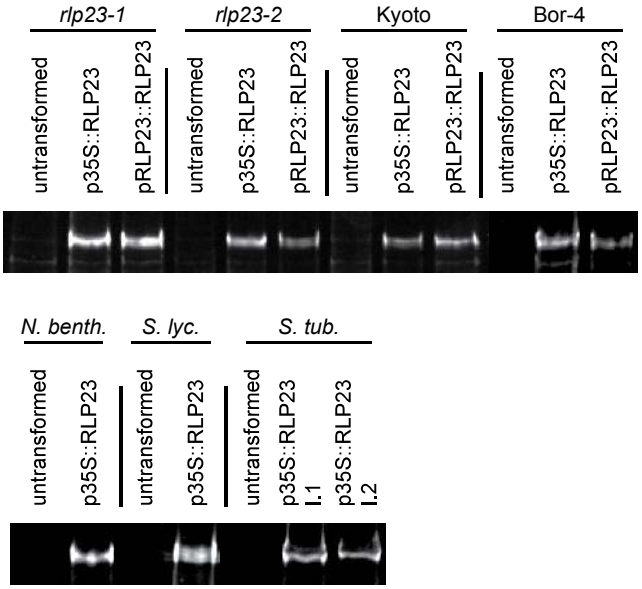
rlp23-1
rlp23-2
Kyoto
Bor-4
untransformed
p35S::RLP23
pRLP23::RLP23
N. benth.
S. lyc.
S. tub.
p35S::RLP23 l.1
p35S::RLP23 l.2

DOI: 10.1038/NPLANTS.2015.140

Supplementary Fig. 4: RLP23 expression analysis in transgenic plants. Protein blot probed with anti-GFP antiserum of protein extracts from *A. thaliana* genotypes *rlp23-1*, *rlp23-2*, *A. thaliana* accessions Kyoto and Bor-4, *N. benthamiana*, *Solanum lycopersicum* and *Solanum tuberosum* plants stably producing GFP-tagged RLP23 protein.

Fig. S5

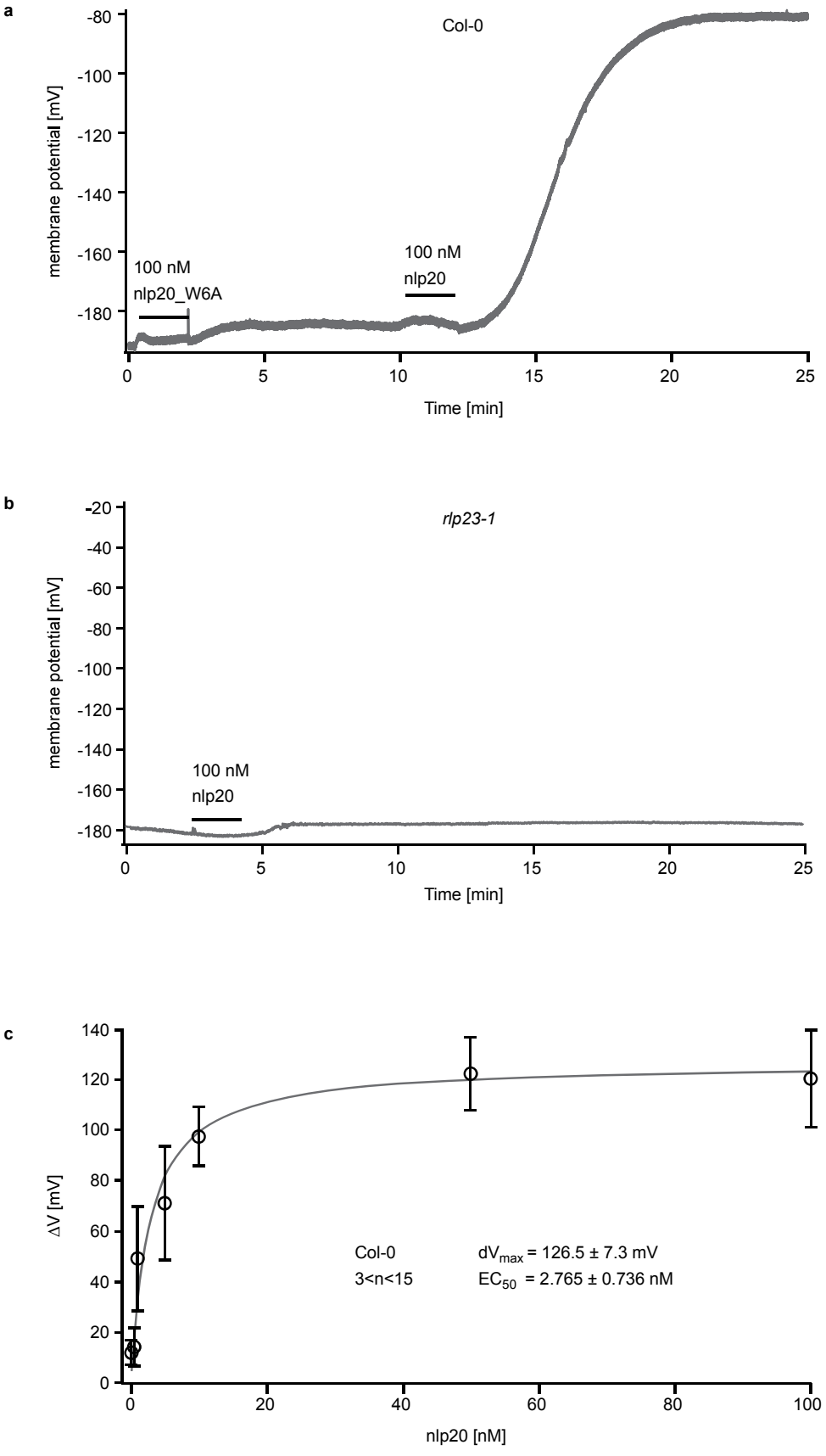
a
Col-0
membrane potential [mV]
-80
-100
-120
-140
-160
-180
100 nM
nlp20_W6A
100 nM
nlp20
0
5
10
15
20
25
Time [min]
b
rlp23-1
membrane potential [mV]
-20
-40
-60
-80
-100
-120
-140
-160
-180
100 nM
nlp20
0
5
10
15
20
25
Time [min]
c
ΔV [mV]
140
120
100
80
60
40
20
0
Col-0
3<n<15
dV$_{max}$ = 126.5 ± 7.3 mV
EC$_{50}$ = 2.765 ± 0.736 nM
0
20
40
60
80
100
nlp20 [nM]

DOI: 10.1038/NPLANTS.2015.140

Supplementary Fig. 5: Plasma membrane depolarisation in *Arabidopsis thaliana* Col-0 and *rlp23-1* plants. a, **b**, Plasma membrane depolarisation in leaf cells from *A. thaliana* Col-0 WT plants and *rlp23-1* plants following perfusion with 100 nM nlp20 and inactive nlp20_W6A. Bars indicate time intervals of elicitor application. **c**, Half maximum effective concentration for membrane depolarisation is indicated.

Fig. S6

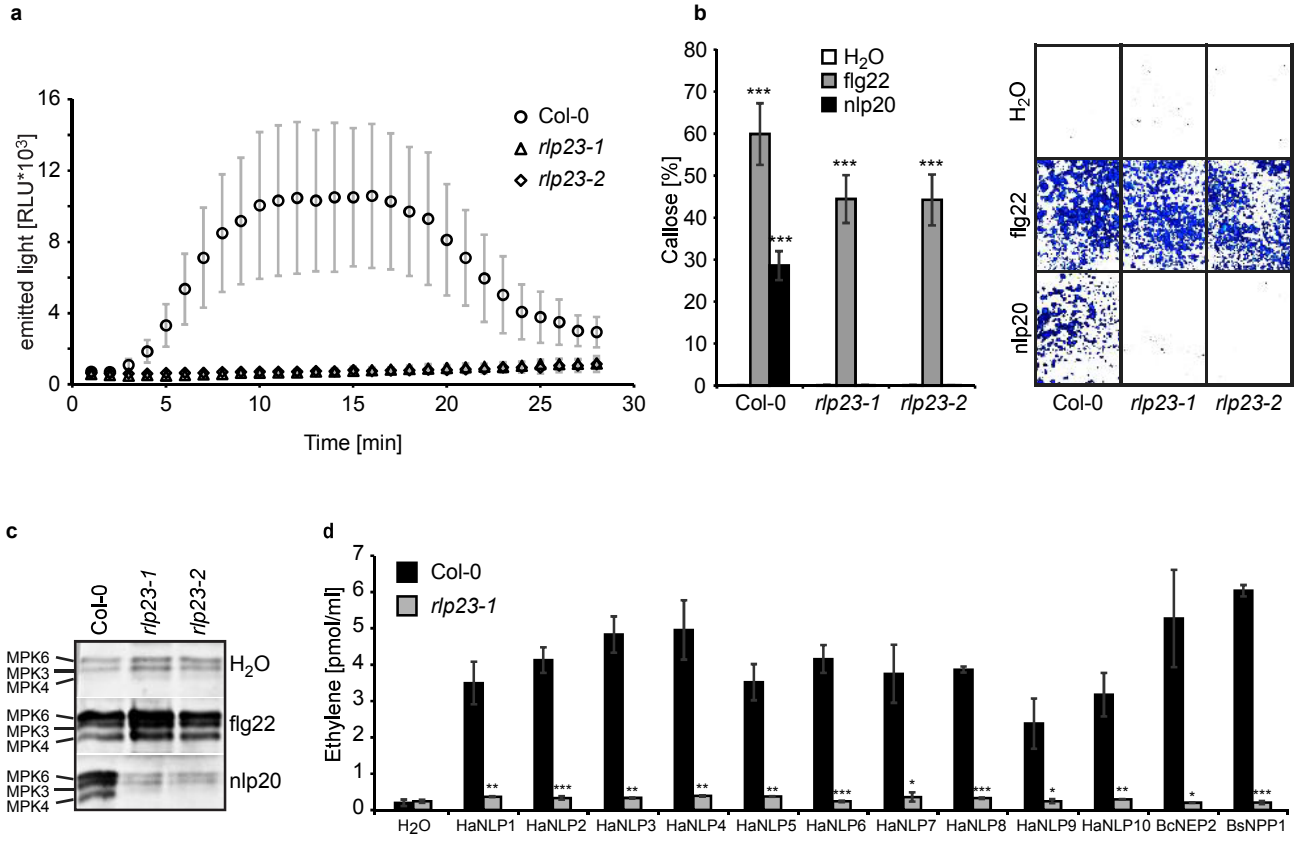
a
emitted light [RLU*10³]
Time [min]
Col-0
rlp23-1
rlp23-2
b
Callose [%]
H2O
flg22
nlp20
Col-0
rlp23-1
rlp23-2
c
MPK6
MPK3
MPK4
H2O
flg22
nlp20
d
Ethylene [pmol/ml]
H2O
HaNLP1
HaNLP2
HaNLP3
HaNLP4
HaNLP5
HaNLP6
HaNLP7
HaNLP8
HaNLP9
HaNLP10
BcNEP2
BsNPP1

DOI: 10.1038/NPLANTS.2015.140

Supplementary Fig. 6: Nlp20-mediated defense responses are impaired in *rlp23* mutants. a, Oxidative burst triggered by nlp20 (1 µM). **b**, Callose apposition triggered by 1 µM nlp20. **c**, MAPK activation triggered by 1 µM nlp20. Water and flg22 (1 µM) were used as controls (**b**, **c**). **d**, Ethylene accumulation upon treatment with nlp24 peptides derived from various NLPs of *Hyaloperonospora arabidopsidis* (*Ha*NLP3), *Botrytis cinerea* (*Bc*NEP2), and *Bacillus subtilis* (*Bs*NPP). Results represent average values of 3 replicates ± standard deviation. Asterisks indicate significant differences to water treatment (* = P<0.05, ** = P<0.01, *** = P<0.001, Students t-test). All experiments were performed in triplicate with similar results.

Fig. S7

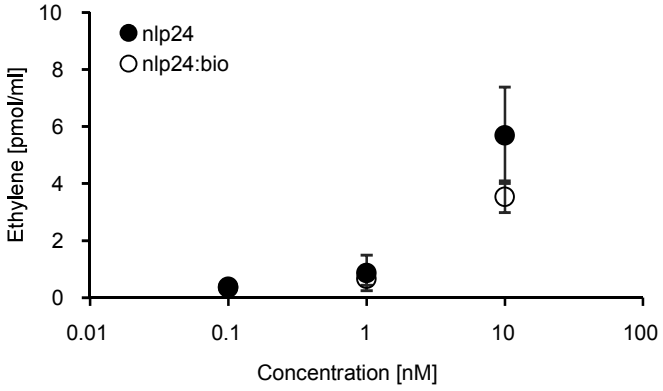
nlp24
nlp24:bio
Ethylene [pmol/ml]
10
8
6
4
2
0
0.01
0.1
1
10
100
Concentration [nM]

DOI: 10.1038/NPLANTS.2015.140

Supplementary Fig. 7: Biotinylated nlp24 peptide is biologically active.

Ethylene accumulation in *Arabidopsis* (Col-0) leaves treated with biotinylated nlp24 (nlp24:bio) and nlp24 (*Pp*NLP). Data points represent means of three replicates ± SD.

Fig. S8

a

genotype		WT	*rlp23-1/* p35S::RLP23:GFP	
treatment		+nlp20	-nlp20	+nlp20
number of peptides per protein	RLP23:GFP	0	35	34
	SOBIR1	1	15	15
	BAK1	0	0	3

b

rlp23-1/35S::RLP23:GFP -nlp20

protein	coverage	peptide sequence	PEP score	frequency
SOBIR1	26.7 %	GSEKPPGPSIFSPLIK	1,84E^{-09}	2
		DLKPANVLLDDDMEAR	2,67E^{-08}	1
		ALQVIETELGVNSQR	1,16E^{-07}	1
		SEINTVGHIR	3,60E^{-05}	1
		IACYCTLDDPK	6,40E^{-05}	1
		DADELTDEDSK	0,00088055	1
		NIITSENPSLAIDPK	0,0013076	3
		SSASDVNPCGR	0,0057918	1
		YLEGPAPVMSSIK	0,0087263	2
		LMDQGFDEQMLLVLK	0,025054	2
		LSGNLNFLK	0,042641	1
		LIIQAIR	0,058667	1
		TMLSQIK	0,059334	1
		GGCGEVFK	0,092929	1
		RGVFCER	0,1067	1

rlp23-1/35S::RLP23:GFP +nlp20

protein	coverage	peptide sequence	PEP score	frequency
BAK1	5 %	GFCMTPTER	0,012288	1
		LADGTLVAVK	0,014127	1
		LANDDDVMLLDWVK	0,076058	1
SOBIR1	26.4 %	NIITSENPSLAIDPK	5,65E^{-10}	4
		GSEKPPGPSIFSPLIK	1,60E^{-09}	1
		IACYCTLDDPK	4,77E^{-07}	1
		DLKPANVLLDDDMEAR	3,39E^{-06}	4
		SEINTVGHIR	7,65E^{-06}	1
		YLEGPAPVMSSIK	0,00057632	2
		SSASDVNPCGR	0,0055006	1
		DADELTDEDSK	0,0056767	1
		ILDLSSNK	0,00872	1
		ALQVIETELGVNSQR	0,014284	1
		HSATTGEYVLR	0,063185	1
		TMLSQIKH	0,074387	1
		LSGNLNFLK	0,08528	1
		RGVFCER	0,12811	1
		GGCGEVFK	0,14319	1

c

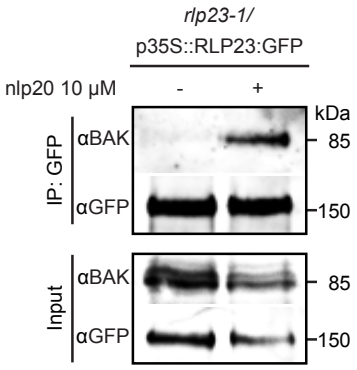

DOI: 10.1038/NPLANTS.2015.140

Supplementary Fig. 8: Identification of SOBIR1 and BAK1 fragments after RLP23:GFP pull-down in LC-MS/MS Analyses and pull-down of endogenous BAK1 in *Arabidopsis*. **a**, Stably transformed *rlp23-1/p35S::RLP23:GFP* plants treated with nlp20 (1 μM) were used to precipitate proteins interacting with RLP23 using a GFP-trap. Interacting proteins were identified by LC-MS/MS. Number of peptides representing RLP23 interactors SOBIR1 and BAK1 are given. **b**, overview on SOBIR1 and BAK1-derived peptides identified by MS/MS analysis. Peptide sequences, protein coverage and peptide frequencies are given. **c**, Co-immunoprecipitation of endogenous BAK1 in a ligand-dependent manner (10 μM nlp20) in *Arabidopsis* plants stably expressing 35S::RLP23:GFP using GFP-trap beads. Western blots were probed with antisera specific for BAK1 or GFP respectively.

Fig. S9

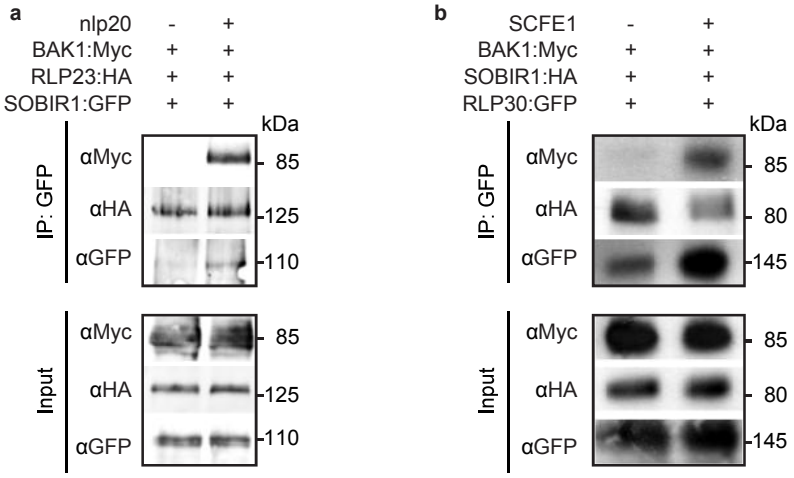
a
nlp20 - +
BAK1:Myc + +
RLP23:HA + +
SOBIR1:GFP + +
kDa
IP: GFP
αMyc
αHA
αGFP
85
125
110
Input
αMyc
αHA
αGFP
85
125
110
b
SCFE1 - +
BAK1:Myc + +
SOBIR1:HA + +
RLP30:GFP + +
kDa
IP: GFP
αMyc
αHA
αGFP
85
80
145
Input
αMyc
αHA
αGFP
85
80
145

DOI: 10.1038/NPLANTS.2015.140

Supplementary Fig. 9: RLP23 and RLP30 recruit BAK1 in a ligand-dependent fashion. **a, b,** Pull down of BAK1:Myc transiently co-expressed with SOBIR1:GFP and RLP23:HA (**a**) or SOBIR1:HA and RLP30:GFP (**b**) in *N. benthamiana* plants upon leaf infiltration with 1 μM nlp20 (**a**) or SCFE1 elicitor[15] (**b**). Protein extracts were subjected to co-immunoprecipitation using GFP-trap beads and SDS-PAGE/blotting. Protein blots were probed with tag-specific antisera. Representative blots of at least two independent repetitions are shown.

Fig. S10

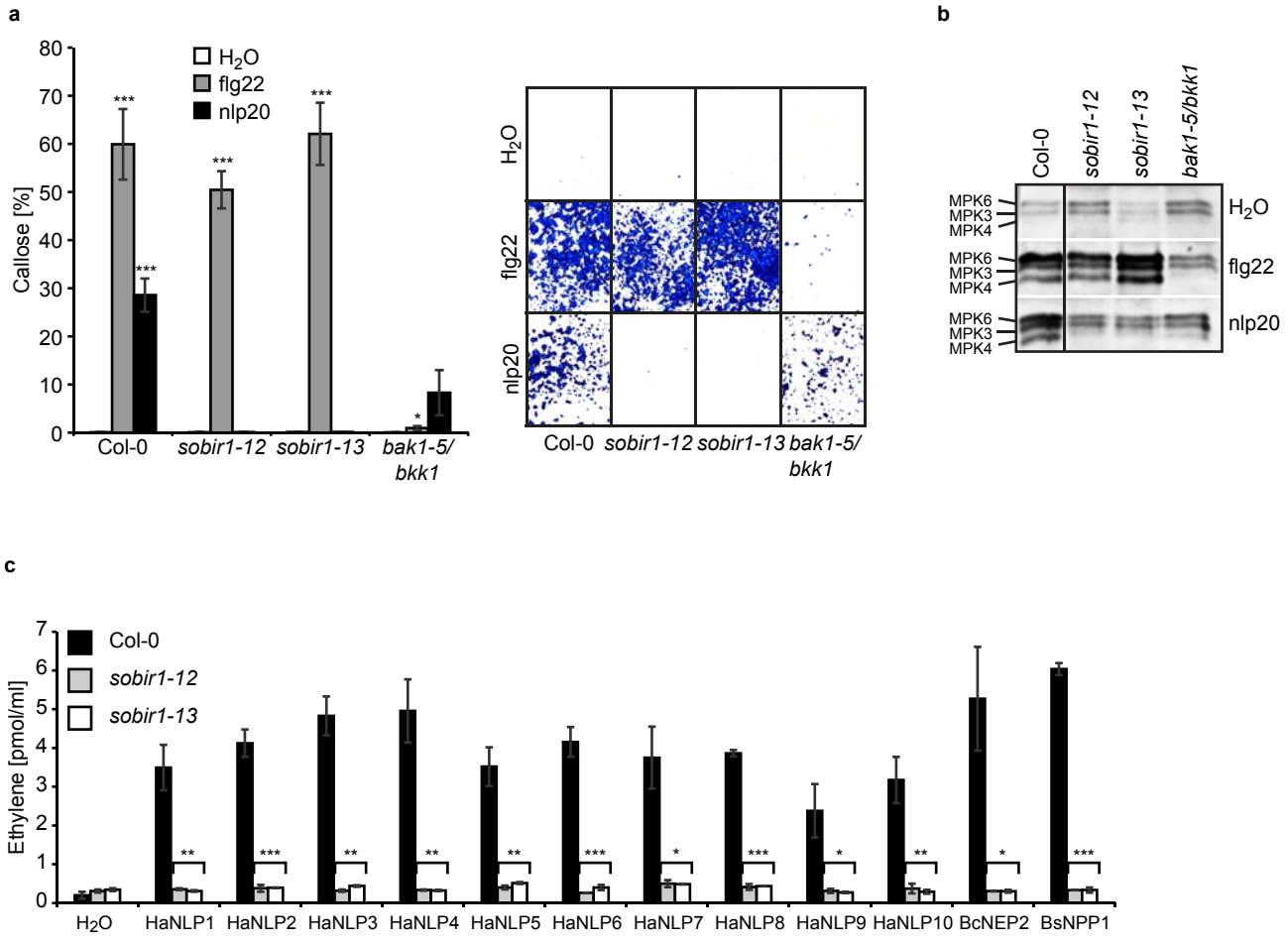
a
Callose [%]
H2O
flg22
nlp20
Col-0
sobir1-12
sobir1-13
bak1-5/bkk1
b
Col-0
sobir1-12
sobir1-13
bak1-5/bkk1
MPK6
MPK3
MPK4
H2O
flg22
nlp20
c
Ethylene [pmol/ml]
Col-0
sobir1-12
sobir1-13
H2O
HaNLP1
HaNLP2
HaNLP3
HaNLP4
HaNLP5
HaNLP6
HaNLP7
HaNLP8
HaNLP9
HaNLP10
BcNEP2
BsNPP1

DOI: 10.1038/NPLANTS.2015.140

Supplementary Fig. 10: nlp20-mediated responses are impaired in *sobir1* and *bak1-5/bkk1* mutants. a, Callose apposition triggered by 1 μM nlp20. **b**, MAPK activation triggered by 1 μM nlp20. Flagellin (1 μM) or water was used as positive or negative controls, respectively. **c**, Ethylene accumulation upon treatment with nlp24 peptides derived from various NLPs of *Hyaloperonospora arabidopsidis*, *Botrytis cinerea* (*Bc*NEP2), and *Bacillus subtilis* (*Bs*NPP1). Results represent average values of 3 replicates ± standard deviation. Asterisks indicate significant differences to water control treatments (* = P<0.05, ** = P<0.01, *** = P<0.001, Student's t-test). Experiments were done in triplicate with similar results.

Fig. S11

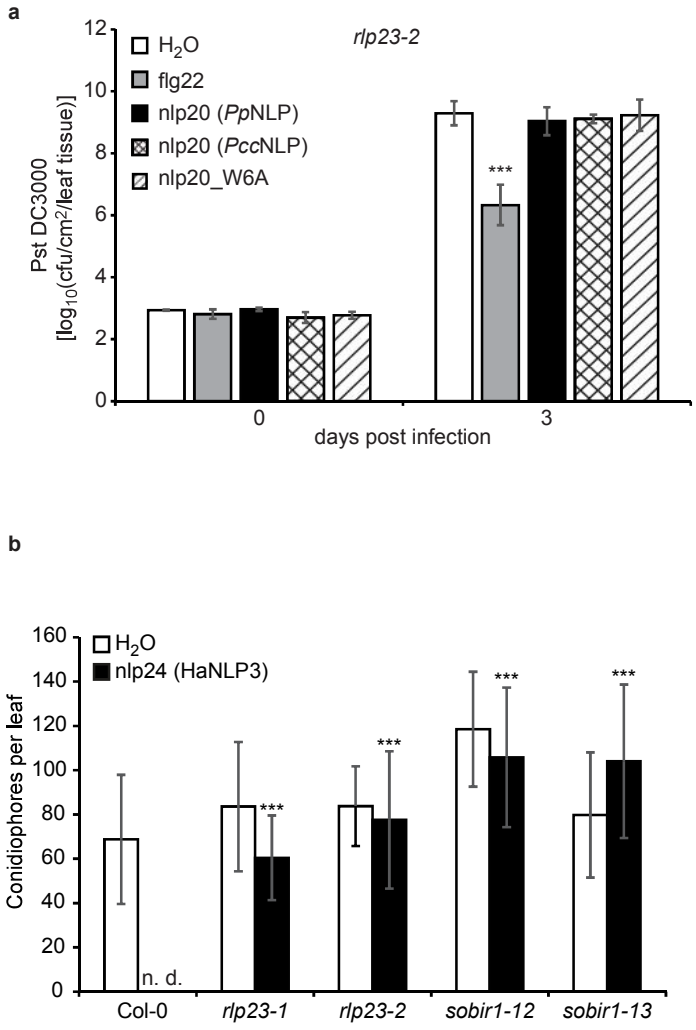
a
rlp23-2
H2O
flg22
nlp20 (PpNLP)
nlp20 (PccNLP)
nlp20_W6A
Pst DC3000
[log10(cfu/cm2/leaf tissue)]
12
10
8
6
4
2
0
***
0
3
days post infection
b
H2O
nlp24 (HaNLP3)
Conidiophores per leaf
160
140
120
100
80
60
40
20
0
n. d.
***
***
***
***
Col-0
rlp23-1
rlp23-2
sobir1-12
sobir1-13

DOI: 10.1038/NPLANTS.2015.140

Supplementary Fig. 11: RLP23 and SOBIR1 mediate local immunity. a, Growth of *Pseudomonas syringae* pv. *tomato* on *rlp23-2* leaves primed for immunity by treatments with nlp20 (*Pp*NLP), flg22, or immunogenically inactive peptides nlp20 (*Pcc*NLP) and nlp20_W6A (1 µM) 24 hrs prior to infection. Water infiltration served as control. Data represent means ± SD of n = 6 plants per treatment. **b**, Growth of *Hyalonospora arabidopsidis* isolate Noco2 on leaves of *A. thaliana* Col-0, *rlp23* and *sobir1* mutant genotypes treated with nlp24 (*Ha*NLP3) (100 nM) or water as control 24 hrs prior to infection. Conidiospores were counted 6 days post inoculation. Data represent means ± SD of 16<n<32 leaves per treatment. Asterisks indicate significant differences to control treatments (**a**) or to Col-0 plants (**b**) (*** = P<0.001, Student's t-test).

Fig. S12

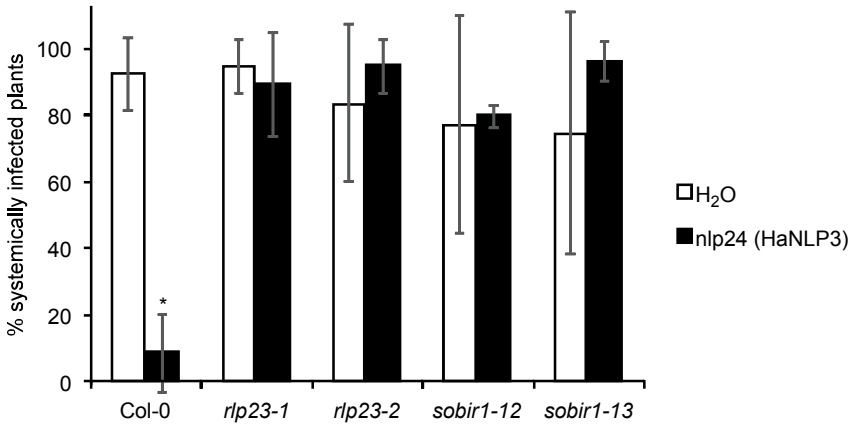
% systemically infected plants
100
80
60
40
20
0
*
Col-0
rlp23-1
rlp23-2
sobir1-12
sobir1-13
H2O
nlp24 (HaNLP3)

DOI: 10.1038/NPLANTS.2015.140

Supplementary Fig. 12: RLP23 and SOBIR1 mediate systemic immunity. Leaves of *A. thaliana* Col-0, *rlp23* and *sobir1* mutant genotypes were treated with nlp24 (*Ha*NLP3) (100 nM) or water as control 24 hrs prior to infection of neighboring, systemic leaves with *H. arabidopsidis* isolate Noco2. Conidiospores were counted 6 days post inoculation. Data represent means ± SD of three independent experiments. The asterisk indicates a significant difference to control treatment (* = P<0.1, Student's t-test).